PNAS RESEARCH ARTICLE | MEDICAL SCIENCES OPEN ACCESS

Pathogens spread by high-flying wind-borne mosquitoes

Roland Bamou[a], Adama Dao[b], Alpha S. Yaro[b], Cedric Kouam[a], Koray Ergunay[c], Brian P. Bourke[c], Moussa Diallo[b], Zana L. Sanogo[b], Samake Djibril[b], Yaw A. Afrane[d], Abdul Rahim Mohammed[d,e], Christopher M. Owusu-Asenso[d], Gabriel Akosah-Brempong[d,f], Cosmos M. Pambit-Zong[d], Benjamin J. Krajacich[a], Roy Faiman[a], M. Andreina Pacheco[g], Ananias A. Escalante[g], Scott C. Weaver[h,i], Rita Nartey[a], Jason W. Chapman[j,k], Don R. Reynolds[l,m], Yvonne-Marie Linton[c], and Tovi Lehmann[a,1]

Affiliations are included on p. 7.

Edited by Anthony James, University of California Irvine, Irvine, CA; received May 29, 2025; accepted September 12, 2025

Mosquito-borne diseases such as malaria and dengue threaten billions of people and cause the death of hundreds of thousands annually. Recent studies have revealed that many mosquito species regularly engage in high-altitude wind-borne migration, but its epidemiological significance remains unclear. The hypothesis that high-flying mosquitoes spread pathogens over long distances has not been directly tested. Here, we report that high-flying mosquitoes are commonly infected with arboviruses, protozoans, and helminths and provide a insights into this pathogen–vector aerial network. A total of 1,017 female mosquitoes intercepted on nets suspended from helium balloons at 120 to 290 m above ground over Mali and Ghana were screened for infection with arboviruses, Haemosporida, and filariae. The mosquitoes collected at altitude comprised 61 species, across 10 genera, dominated by *Culex*, *Aedes,* and *Anopheles*. Infection and infectiousness (capacity to transmit a pathogen to another host inferred based on disseminated infection) rates of migrant mosquitoes were 7.2% and 4.4% with *Plasmodium* spp., 1.6% and 0.6% with filariae, and 3.5% and 1.1% with flaviviruses, respectively. Twenty-one mosquito-borne pathogens were identified, including Dengue, West Nile, and M'Poko viruses, 15 avian *Plasmodium* species including *Plasmodium matutinum*, and three filariids, including *Pelecitus* sp. Confirmed head–thorax (disseminated) infections of multiple pathogens in *Culex perexiguus*, *Mansonia uniformis*, and *Anopheles squamosus* reveal that pathogens carried by high-altitude wind-borne mosquitoes are capable of infecting hosts far from their departure location. This high-altitude traffic of sylvatic pathogens (circulating in wild animals) may be key to their maintenance among enzootic foci as well as initiating outbreaks at distant locations.

mosquito-borne pathogen | dispersal | disease-spread | high-altitude windborne migration | disease surveillance

Significance

Mosquito-borne diseases threaten public health and food security. Long-range spread of these pathogens has been regarded as reflecting human or animal movement. By screening approximately one thousand mosquitoes captured on nets suspended from helium balloons at 120 to 290 m above ground, we detected high rates of infection with arboviruses, protozoans, and helminths. Twenty-one mosquito-borne pathogens of vertebrates were identified including Dengue, West Nile and M'Poko viruses, *Plasmodium matutinum*, and *Pelecitus* spp. Disseminated infections indicate that a substantial proportion of high-flying mosquitoes are likely capable of infecting hosts far from their departure location. Traffic of sylvatic pathogens (circulating among wild animals) at altitude may be key to their maintenance among disease foci and for initiating outbreaks at distant locations, as well as to disease prevention and control.

Wind-borne insect migration at altitude occurs regularly on massive scales in terms of biomass and distance that extend up to hundreds of kilometers per night (1–6). Migration, defined as a persistent movement temporarily unaffected by immediate cues for food, reproduction, or shelter, with a high probability of relocating the animal to a new environment (7, 8) fits these flights and will be used here. Insects that transmit pathogens, other pests, and species vital for ecosystem vigor are common among high-altitude flyers (1–3, 5, 6). However, migrations in tropical mosquitoes are poorly understood and questions about their effects on mosquito survival, reproduction, range expansion, spread of insecticide resistance, and epidemiology of vector-borne diseases remain enigmatic despite their potentially large impacts (9–16). The hypothesis of pathogen spread by high-altitude wind-borne mosquitoes is not new (2, 11, 17–24), but it has been supported largely by epidemiological and meteorological inferences, while direct evidence of the regularity of such movements, particularly of the infection of high-altitude wind-borne mosquitoes, has been elusive. Recent studies in Africa revealed that many mosquito species engage in wind-borne migration at altitude, i.e., 40 to 290 m above ground level (agl), on a regular basis (25–27) along with myriads of other insects (3, 28). Additional support for this hypothesis was provided by the findings that the migrants were dominated by gravid females that had fed on vertebrate blood before engaging in migratory flight, that the flights coincided with the disease-transmission season, and that many of these species have been previously implicated as vectors of pathogens (15, 25, 26). Here, we show that high-flying migrant mosquitoes of diverse taxa are often infected with arboviruses, *Plasmodium* spp., and filariae. Furthermore, migrating mosquitoes are not only infected i.e., exposed to these pathogens, but are already likely infectious, i.e., presenting a disseminated infection to the haemocoel and likely to the salivary glands, highlighting their probable capacity to transmit pathogens upon landing in a distant territory.

The authors declare no competing interest.

This article is a PNAS Direct Submission.

[1] To whom correspondence may be addressed. Email: tlehmann@niaid.nih.gov.

This article contains supporting information online at https://www.pnas.org/lookup/suppl/doi:10.1073/pnas.2513739122/-/DCSupplemental.

Published November 25, 2025.

Results

Aerial Mosquito Diversity. Of 1,247 mosquitoes collected at altitude (120 to 290 m agl) over West Africa during 191 collection nights between 2018 and 2020 and subjected to molecular analysis, the specific identity of 994 mosquitoes were confirmed by mitochondrial cytochrome c oxidase I (*COI*) barcode sequencing (253 were identified to subfamily; *SI Appendix*, Table S1), yielding 61 species across 10 genera (Fig. 1 and *SI Appendix*, Table S1). Diversity of *Culex* was highest (25 species), followed by *Anopheles* (11 species), *Aedes* (10 species), *Coquillettidia* (4 species), *Uranotaenia* (3 species), *Mansonia* (3 species), *Mimomyia* (2 species), *Eretmapodites* (1 species), *Aedeomyia* (1 species), and *Lutzia* (1 species). Among those identified to species, *Culex watti, Culex perexiguus,* and *Cx. cf. watti MAFP5.C5* were the dominant taxa, comprising nearly 60% of the collections, followed by nine species, including *Coquillettidia metallica*, *Culex univittatus*, *Aedes argenteopunctatus,* and *Anopheles squamosus*, which together comprised a further 20% of the collections (Fig. 1*A*). Infrequent taxa included 32 species, e.g., each represented by 0.2 to 1.2% of the specimens (2 to 12 specimens/species); followed by 17 rare species, each represented by a single specimen (singletons, Fig. 1 and *SI Appendix*, Fig. S1). Identified taxa included primary vectors of malaria (*Anopheles coluzzii, Anopheles gambiae* s.s.) and arboviruses, e.g., West Nile virus (WNV, species *Orthoflavivirus nilense,* vectored by *Cx. univittatus*), and Rift Valley fever virus (species *Phlebovirus riftense*, vectored by *Aedes mcintoshi*) (15, 29–31). Females comprised 81% of identified specimens, with no evidence for interspecies heterogeneity in the sex composition (P = 0.065, Exact Test for contingency tables, *SI Appendix*, Table S2). Overall, gravid females consisted of 43% of identified species with fractions varying between 28% (*Aedes circumluteolus*, N = 10) to 65% (*An. squamosus*, N = 17, among-species heterogeneity P = 0.001, Exact Test for contingency tables, *SI Appendix*, Table S3).

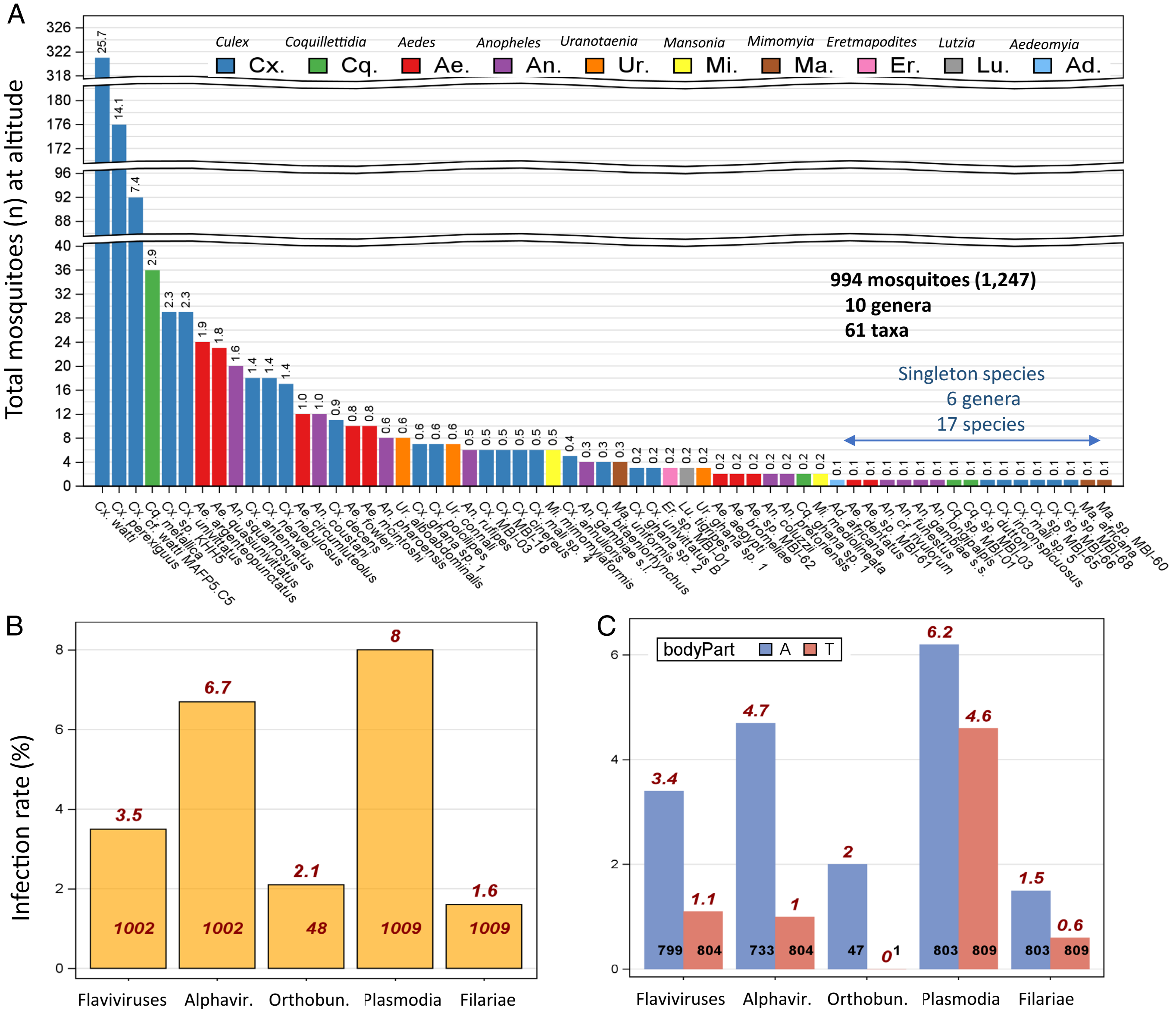

Fig. 1. Mosquito species composition at altitude and overall infection rates with major pathogen groups. (*A*) Mosquitoes identified to species are shown (N = 994, note breaks in the Y-axis; showing the number of specimens per species). The percentage of the total specimens per species is shown above bars. Species represented by a single specimen are grouped under the blue arrow. (*B*) Overall infection rates (per mosquito) of high-altitude wind-borne mosquitoes with pathogen groups assayed. (*C*) Infection rate in abdominal tissues (A, blue) and in head–thorax tissues (T, red). Infection rates expressed as percentages are shown above bars (red), and corresponding sample sizes are shown at the base.

Table 1. Overall infection rates of mosquito females intercepted at altitude (120 to 290 m above ground) with pathogens

Pathogen (lineage)	Overall[*] (N)	Abdomen (N)	Head–thorax (N)	Method[†]	Hosts[‡]	Human impact[§]
Flaviviruses	3.5% (35/1,002)	3.4% (27/799)	1.1% (9/804)	Pan-Flavi	V/A	H, L [Z,P]
West Nile Virus (1a)[¶]	0.2% (2/1,002)	0.25% (2/799)	0% (804)	Sanger	B/M	H, L [Z]
Dengue (2)[#]	0.2% (2/1,002)	0.25% (2/799)	0% (804)	Sanger	P/M	H, P [P]
Peribunyaviridae; Orthobunyavirus	2.1% (1/48)	2.1% (1/47)	0% (1)	Metagen	V/A	H, L [Z]
M'Poko virus[||]	2.1% (1/48)	2.1% (1/47)	0% (1)	Metagen	B/M	H [Z]
Alphaviruses[**]	6.7% (67/1,002)	1.0% (8/799)	4.7% (38/804)	Pan-Alpha	V/A	H, L [Z]
Plasmodia[††]	8.0% (81/1,009)	6.2% (50/803)	4.6% (37/809)	Pan-Plasm	B/A	H [P,Z]
P. AFR006	0.1% (1/1,009)	0% (0/803)	0.1% (1/809)	Sanger	B/M	N
P. AFR146	0.2% (2/1,009)	0% (0/803)	0.3% (2/809)	Sanger	B/M	N
P. GBCAM1	0.3% (3/1,009)	0.25% (2/803)	0.1% (1/809)	Sanger	B/M	N
P. CAMBRA02	0.1% (1/1,009)	0.1% (1/803)	0% (0/809)	Sanger	B/M	N
P. TCHSEN01	0.2% (2/1,009)	0.25% (2/803)	0.0% (0/809)	Sanger	B/M	N
P. CXPER01	1.1% (12/1,009)	0.6% (5/803)	0.5% (4/809)	Sanger	B/M	N
P. matutinum (VETMED)	3.1% (31/1,009)	1.5% (12/803)	2.1% (17/809)	Sanger	B/M	N
P. relictum (SGS1)	0.1% (1/1,009)	0% (0/803)	0.1% (1/809)	Sanger	B/M	N
P. vaughani (SYAT05)	0.6% (6/1,009)	0.6% (5/803)	0.1% (1/809)	Sanger	B/M	N
P. MALNI02[‡‡]	0.1% (1/1,009)	0.1% (1/803)	0% (0/809)	Sanger	B/M	N
P. AEDMCI01[§§]	0.1% (1/1,009)	0.1% (1/803)	0% (0/809)	Sanger	B/M	N
P. CULWAT01[§§]	0.1% (1/1,009)	0.1% (1/803)	0% (0/809)	Sanger	B/M	N
P. AEDQUA01[§§]	0.1% (1/1,009)	0.1% (1/803)	0% (0/809)	Sanger	B/M	N
P. CULANN01[§§]	0.1% (1/1,009)	0.1% (1/803)	0% (0/809)	Sanger	B/M	N
P. Ghana sp. 1[§§]	0.1% (1/1,009)	0% (0/803)	0.1% (1/809)	Sanger	B/M	N
Filariae (Onchocercidae)	1.6% (16/1,009)	1.5% (12/803)	0.6% (5/809)	Pan-Filari	V/A	H, L
Cardiofilaria sp.	0.1% (1/1,009)	0.1% (1/803)	0% (0/809)	Sanger	B/M	N
Loa-like sp.	0.1% (1/1,009)	0.1% (1/803)	0% (0/809)	Sanger	U/U	N
Pelecitus sp.	0.1% (1/1,009)	0.1% (1/803)	0% (0/809)	Metagen	B,M/M	H [Z]

[*] Mosquito infection rate (regardless of bodypart, including whole-body mosquitoes) using PCR and metagenomics (positives/number tested).
[†] Pan-Flavi = Pan-Flavivirus RT-qPCR; Metagen = Metagenomics; Pan-Alpha = Pan-Alphavirus RT-qPCR; Pan-Plasmo = Pan-Plasmodium qPCR; Pan-Filari = Pan-Filariae qPCR.
[‡] V/A = vertebrate/arthropod; B/A = bird/arthropod; B/M = bird/mosquito; P/M = primate/mosquito; B,M/M = bird+mammal/mosquito; U/U = unknown/unknown.
[§] Direct effect on human (H) or livestock (L) health [P and Z denote human as primary and zoonotic host, respectively]; N = none.
[¶] One mosquito infection confirmed by Sanger (lineage 1a); other infection confirmed by WNV-specific qPCR (not sequencing or metagenomics).
[#] Infection was detected in one mosquito abdomen and another whole-body female.
[||] Infection was detected and confirmed by metagenomics after it was detected as positive to flaviviruses.
[**] Infection with alphaviruses could not be confirmed by Sanger sequencing (N = 67) nor by NGS metagenomics (N = 48).
[††] Putative species names follow most similar sequenced isolate names in MalAvi that were clustered together by the software ASAP (*Materials and Methods*).
[‡‡] Samples with apparent mixed infection, which may result in "chimeric sequences."
[§§] New putative species based on their dissimilarity with nearest matches in the MalAvi database that were clustered separately by ASAP (*Materials and Methods*). Naming follows MalAvi convention: 3 letters of the host genus and species names followed by number (*SI Appendix*, Fig. S2).

Aerial Pathogen Diversity. Pan-genus qPCR/PCR detection assays targeting Haemosporida, filariae, flaviviruses, and alphaviruses were performed on 1,009 female mosquitoes that were captured at altitude, consisting of 803 abdomens, 809 thoraxes, and 194 whole-body specimens. Overall mosquito infection rates (infection of any mosquito part) with each pathogen group varied between 1.6% (filariae) and 8.0% (*Plasmodium* spp.; Fig. 1*B*, Table 1, and *SI Appendix*, Table S4). Infection rates for flaviviruses, *Plasmodium* spp., and filariae were higher in abdominal tissues than in head–thorax tissues (Fig. 1*B* and Table 1), probably reflecting residual pathogen DNA/RNA after exposure via bloodmeal (see also *SI Appendix*, Table S4) and early infection before pathogen dissemination beyond the midgut (abdomen) (32, 33). Sequence data confirmed pathogen infections in high-altitude mosquitoes with all pathogen groups except alphaviruses; hence, alphaviruses were excluded from subsequent analyses.

In addition to target sequencing of positive mosquitoes following qPCR/PCR pathogen detection assays, metagenomic sequences of 48 samples found positives for pan-flavivirus, pan-filaria, and pan-Haemosporida and revealed infection with viruses of other families, as well as with non-mosquito-borne pathogens (Table 1 and *SI Appendix*, Table S4). Overall, a total of 21 mosquito-borne pathogens of vertebrates were detected in this modest sample, including two flaviviruses: WNV and Dengue (DENV, species *Orthoflavivirus dengue*), one orthobunyavirus, M'Poko virus (species *Orthobunyavirus mpokoense*, MPOV), 15 avian *Plasmodium* species (*SI Appendix*, Fig. S2), and three filariid nematodes (Table 1). The *Plasmodium* spp. included the cosmopolitan *Plasmodium matutinum*, *Plasmodium relictum*, and *Plasmodium vaughani* and the African-endemic *P.* MALNI02 previously detected in Blue-billed Malimbe, *Malimbus nitens*, in Gabon (34) (Table 1). The three filarial taxa were members of different genera: *Cardiofilaria* sp., *Pelecitus* sp., as well as a taxon related to the genus *Loa* (Table 1). Natural hosts of these taxa include both birds and mammals (Table 1). These pathogens represent sylvatic (i.e., circulating among wild animals) and zoonotic (transmitted to people from an animal natural host) species, e.g., WNV, which are transmitted by mosquitoes mainly among birds (but see DENV, Table 1). Several insect-specific viruses (viruses that infect insects, but are incapable of infecting vertebrates, e.g., Barkedji virus and Nienokue virus, *SI Appendix*, Table S4), as well as non-mosquito-borne pathogens, e.g., *Trypanosoma theileri* and *Haemoproteus coraciae* were also detected (*SI Appendix*, Table S4). Coinfection between pairs of pathogen groups (flaviviruses, *Plasmodium* spp., and filariid nematodes) did not depart from random expectations when tested in whole body, abdomens, and head–thorax body parts ($P > 0.2$, Fisher exact tests).

Pathogen–Mosquito Relationships. Infection with *Plasmodium* spp., filariae, or flaviviruses based on genus-specific PCR/qPCR was detected in 26 mosquito species intercepted at altitude, with an overall infection rate of 12.7% per female (N = 1,009), 10.7% in abdomens (N = 803), and 6.3% in head–thorax sections (N = 809, Table 1). These rates varied among mosquito species, but no systematic relationships between species' sample size and pathogen prevalence were observed (Fig. 2*A* and *SI Appendix*, Fig. S3). Both *Cx. neavei* and *Ur. connali* exhibited significantly higher overall infection rates than the means across all mosquito species ($P < 0.015$, 1 sided Monte Carlo Exact Tests for contingency tables, Fig. 2*A* and *SI Appendix*, Fig. S3). Importantly, 15 mosquito species exhibited disseminated (head–thorax) infections with these pathogen groups, a condition required for infection of salivary glands and transmission competence (Fig. 2*B* and *SI Appendix*, Fig. S4). Positive relationships between abdominal and head–thorax infection, shown by high values in both axes (Fig. 2*B*) are likely driven by susceptible, competent vectors that are more commonly exposed to these pathogens by preferably feeding on their natural host species. Such species include *Ur. connali*, *Ma. uniformis*, *Cq. metallica*, and *Ae. circumluteolus* (Fig. 2*B* and *SI Appendix*, Fig. S4). *Culex. perexiguus* is mapped close to the regression line, yet with 16% abdominal infection rate and 8% head–thorax (disseminated) infection rate, it is flagged as a vector of potential importance because of its high abundance at altitude (Figs. 1*A* and 2*B* and *SI Appendix*, Fig. S4).

Sequencing of positive mosquitoes revealed 21 mosquito-borne pathogen species (Table 1 and Fig. 2*C*). Pathogen species were often detected in several mosquito species, including in species from different genera (Fig. 2*C*). The average number of mosquito species per pathogen species was 2.1 overall (range 1 to 11), with 1.7 for (vertebrate) arboviruses, 2.1 for avian *Plasmodium*, and 1.0 for filariae. The number of pathogen species detected per mosquito species overall and as disseminated infection increased with the mosquito species sample size (*SI Appendix*, Fig. S5).

Twenty-four mosquito species infected with at least one mosquito-borne pathogen species represented seven genera, with the genus *Culex* comprising half of the species (Fig. 2*C* and *SI Appendix*, Fig. S4). Mosquito-borne pathogen richness in *Cx. perexiguus* (7) was highest, including two arboviruses (WNV, MPOV) and 5 *Plasmodium* species (Fig. 2*C* and *SI Appendix*, Fig. S5). Disseminated infections with one or more pathogens were detected in twelve mosquito species (50%, Fig. 2*C*), with *Cx. perexiguus* exhibiting the highest richness of disseminated infections (4 species; only *Plasmodium* spp. exhibited head–thorax infections; Fig. 2*C*).

Discussion

The old hypothesis that mosquito-borne pathogens are spread over large distances by wind-borne mosquitoes at altitude (2, 8, 17–19, 24, 25, 35) was based on epidemiological and meteorological inferences and on sporadic observations of mosquitoes at altitude (20, 36, 37). It was not widely accepted because it lacked direct evidence for i) the regularity and scales of such movements and

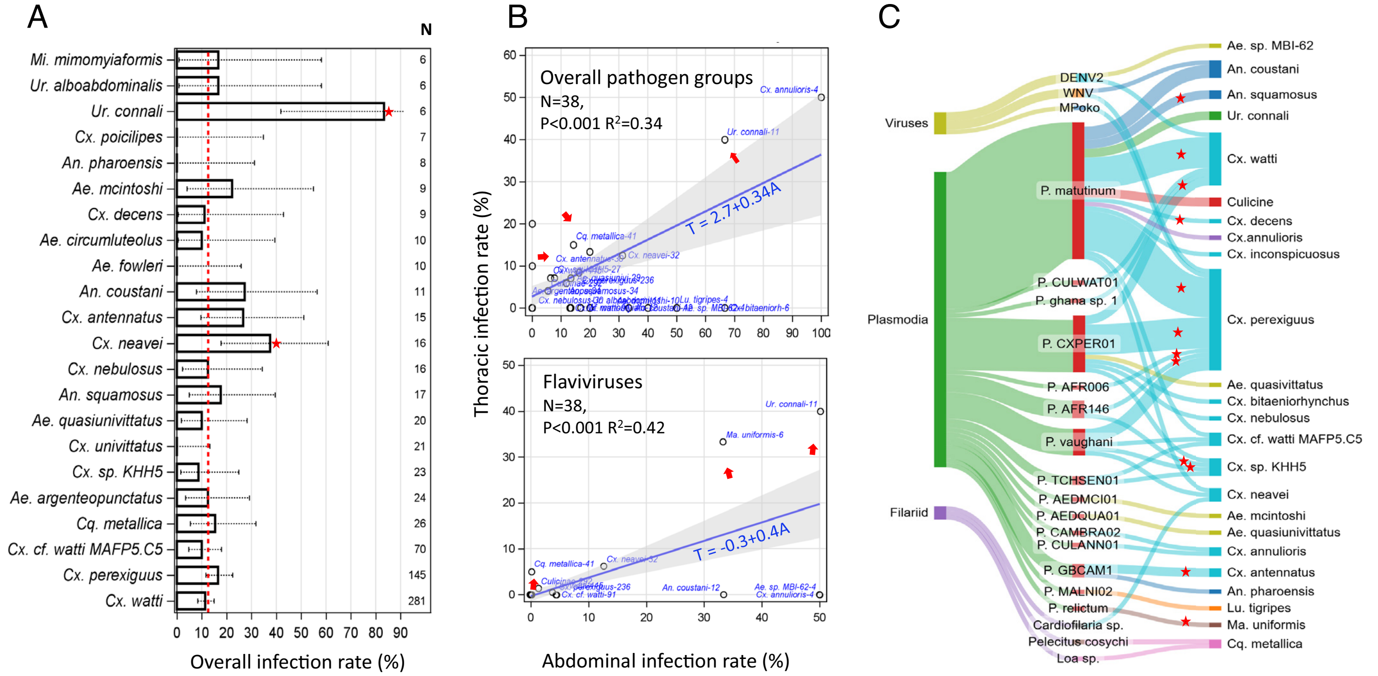

Fig. 2. Overall high-altitude mosquito infection rate per species (*A*), in head–thorax vs. abdominal tissues (*B*), and with specific vertebrate mosquito-borne pathogens (*C*). (*A*) Overall infection rates per mosquito species (N > 5, above bars) based on pan-genus PCR-based assays for flaviviruses, *Plasmodium* spp., and filariae with 90% CI. Higher infection rate ($P < 0.05$, 1-side Monte Carlo Exact Test for contingency tables) than the rate across all mosquito species (12.7%, red line) are indicated by red stars. (*B*) Relationship between disseminated (head–thorax) infection and exposure (abdominal) infection by species (abbreviated species name is followed by their sample size), with linear regression weighted by sample size (blue) and 95% CI as reference to identify outliers (red arrows). Infection with all pathogen groups (*Top*) and with flaviviruses (*Bottom*) are shown (see *SI Appendix*, Fig. S4 for *Plasmodium* and filariae). (*C*) Sankey diagram showing mosquito species infection with pathogens confirmed by sequencing. Connective band thickness is proportional to infection rate. Red stars indicate disseminated infection.

ii) infection with mosquito-borne pathogens in wind-borne mosquitoes at altitude. The notion that long-range insect migration occurs mostly in prereproductive adults (7) has also led to questioning of the role of migrants in pathogen spread. Systematic aerial collections conducted recently over Africa have revealed regular, large-scale wind-borne migration of mosquitoes (25–27), and the current results reveal high rates of mosquito infection with mosquito-borne arboviruses, *Plasmodium* species, and filariae (overall 12.7%). Importantly, high rates of disseminated infections (overall 6.3%) implicated a considerable proportion of these mosquitoes as infectious—ready to transmit pathogens when taking a blood meal after landing (16). Altogether, these results provide compelling evidence for the spread of a wide range of mosquito-borne pathogens at altitude by wind-borne mosquitoes.

Remarkably, 21 mosquito-borne pathogen species were identified from this modest sample size (1,017 female mosquitoes), including arboviruses affecting humans (dengue, West Nile, and M'Poko viruses). Infection, even with macroparasites such as filarial nematodes (Table 1), does not impede mosquitoes from undertaking high-altitude flights, confirming inferences concerning migratory blackflies infected with *Onchocerca volvulus* (38–40). Such high infection rates raise the possibility that pathogens increase migratory activity (41–43). These 21 pathogen species were detected in 24 of 61 mosquito species collected at altitude (39%). Half of these (12 species, 20% of all species) demonstrated disseminated infections (i.e., in head–thorax). Although salivary gland infection barriers can render mosquitoes with disseminated infections unable to transmit, these barriers are rare (44). Moreover, postdissemination barriers to arboviruses reduce the fraction of infectious mosquitoes, yet species that exhibited disseminated infection typically transmitted the virus to a new host (45, 46). These results reveal that wind-borne migration of diverse pathogens is widespread among multiple mosquito vector species, and lays to rest the notion this is a rare event involving one or a few super-spreader mosquitoes (Table 1 and Fig. 2).

The public health and economical importance of wind-borne pathogen spread by mosquitoes depends on the pathogen species composition, which in turn depends on the mosquito species composition, their abundance, and age (past exposure) at altitude. Additionally, it depends on mosquito displacement, which is determined by the wind speed, trajectory, and flight duration, the number of high-altitude journeys (nights) an individual mosquito takes, the selectivity of wind direction, and whether these mosquitoes survive their journey and refeed following their descent. The suitability of the landing destinations for the mosquitoes and the abundance of susceptible hosts there are also important.

The absence of human *P. falciparum* and *P. ovale*, common in people [65% in Mali (47), 73% in Ghana (48)] suggests that the majority of these mosquitoes have fed on animals rather than people. Further, at least 20 of the 21 mosquito-borne pathogen species detected circulate among wild animals and are considered sylvatic, e.g., dengue virus serotype 2 also circulates among nonhuman primates and possibly birds in West Africa (49). This highlights the value of aerial collections in surveillance of sylvatic pathogens that are especially difficult to monitor; many even lack diagnostic assays (15, 50, 51), and providing information on pathogen and vector movement trajectories, putative sources, and destinations (3, 26). Using long-flying drones or towers requires a larger initial investment but will increase collection throughput and may prove cost-effective. Pathogen spread by wind-borne mosquitoes likely connects sylvatic foci and may prevent regional extinction despite fluctuations including loss in some foci (52–55), thus could be playing a role in maintenance of these pathogens. Where these pathogens arrive at the same destinations using migratory birds (56), or human transport (57, 58), the importance of wind-borne mosquito spread diminishes. Nonetheless, wind-borne mosquitoes likely arrive in certain destinations that migratory birds avoid because they are situated away from their flyways (56) or because the bird's journey is often too long compared with the short period of viremia (3 to 6 d), and growing evidence that virus recrudescence is unlikely in birds, thus limiting the chance that an arbovirus will be carried from an origin to distant destination (59). Spring migration northward occurs when density of local vectors is low, diminishing transmission between hosts along the migration route; an obstacle that is circumvented if infected vectors arrive. In contrast to dogma, the evidence linking birds to the spread of arboviruses over medium and large distances is tenuous reflecting our inability to determine whether an infectious bird is a migrant, where it was infected, and will it continue to move (59). Finally, the massive numbers of insect migrants compared with vertebrate migrants (1, 3, 25, 60, 61) (and see below) may outweigh the transmission risk linked to wind-borne vectors even if their rates of infection are an order of magnitude lower than recorded here.

Nineteen of the 21 mosquito-borne pathogens detected in our sample circulate in birds (Table 1). This may reflect the predominance of the genera *Culex* (77% specimens, 40% species, Fig. 1*A* and *SI Appendix*, Table S1) and *Coquillettidia* (4% specimens, 6.5% species, Fig. 1*A* and *SI Appendix*, Table S1) of which many species feed on birds (62). Information on host preference for most species sampled here is scarce, and the authors could not find records on *Cx. watti*, the most sampled species or on *Ur. connali*, which showed the highest rate of infection. While most *Uranotaenia* species examined to date feed primarily upon the blood of amphibians (62), *Ur. mashonaensis* in northern Nigeria bites humans (29%); other mammals (20%), and birds (24%) (63) and *Ur. alboabdominalis* was reported biting man in Uganda (64), suggesting that exposure of *Ur. connali* to mammalian and avian pathogens is plausible. Although prevalence was not related to species sample size (Fig. 2 and *SI Appendix*, Fig. S3), the number of pathogen species detected per mosquito species increased with sample size (*SI Appendix*, Fig. S5), accounting for the predominance of avian pathogens. Sampling larger numbers of species that typically feed on mammals, such as *Aedes* and *Anopheles* (62) will likely increase the representation of mammalian pathogens. Birds can exhibit persistent infections with *Plasmodium* spp. (even over years) and exceptionally high prevalence (>90%) (65).

The bionomics and vector status of *Cx. watti*, the dominant species in our aerial collection, are unknown. It was reported infected with Sindbis virus (66), a zoonotic avian virus. We cannot rule out that *Cx. watti* transmits dengue among various hosts (49), but the detection of DENV in one specimen here is likely due to residual viral RNA from the blood meal of an infected host. *Culex perexiguus* (the 2nd most abundant species) exhibited the highest pathogen richness and the highest number of pathogens with disseminated infections (*SI Appendix*, Fig. S5). Likewise, *Cx. perexiguus* showed relatively high rates of infection and transmission potential (Fig. 2 and *SI Appendix*, Figs. S2 and S4). *Culex perexiguus'* roles in the transmission of WNV, Usutu virus (*Orthoflavivirus usutu*), Bagaza virus (*Orthoflavivirus bagazaense*), Sindbis virus (*Alphavirus sindbis*), and avian *Plasmodium* spp. in Africa, Europe, and the Mediterranean are amply demonstrated (51, 67). Its large geographical range across Africa, southern Europe, and Asia (15, 68) may well be related to its extensive migratory behavior (Fig. 1 and see ref. 26); and both traits may explain its high infection rate. Because the community of wind-borne mosquito species (>60, Fig. 1*A*) feed on a diverse set of vertebrate species (62, 69), they are likely to spread diverse mosquito-borne pathogens (15, 29, 50). The sizable fraction of pathogens that could be identified only to genus level, without a close match in available databases (*SI Appendix*, Fig. S2 and Tables S1 and S4) suggests that the actual aerial pathogen (and mosquito) diversity is considerably larger.

Estimates of the species' aerial densities reveal that a panel density (*Materials and Methods*) of a single mosquito throughout our study (191 collection nights), is equivalent to an aerial density of 1 female mosquito/390 million m^3 of air. Because nocturnal migration of wind-borne insects at altitude advances in broad fronts, at least tens of kilometers wide (1, 28, 70), the corresponding number of mosquitoes expected to cross a sector of 100 km line perpendicular to the wind direction between 100 and 300 m agl is 11,635 per night. Accordingly, during a migration season of 4 mo, >1 million mosquitoes of each of the 17 rarest species fly at altitude over that sector alone, while the corresponding values are 10 to 200 million for each of the 12 most common species. Using a conservative disseminated infection rate of 0.1% (0.1 to 4.6%, Table 1) implies thousands to millions of potentially infectious high-flying mosquitoes per species crossing each 100 km sector. In tropical regions, mosquitoes are likely to survive a night flight at 100 to 300 m where temperature (mean = 27 °C; range = 24 to 29 °C) and RH (mean = 65%; range = 50 to 81%) are favorable (3) and predators, e.g., birds, bats, and spiders are uncommon (71). Survival in mosquitoes subjected to high altitude conditions was high (92% for 6 h). Subsequently, they laid eggs and took a bloodmeal on par with controls (16, 27), confirming 97% survival of insects collected at altitudes in nonsticky nets, which were able to feed and reproduce (72). Mosquitoes can cover tens to hundreds of kilometers per night (25). Such massive pathogen pressures may greatly exceed the numbers of infectious terrestrial hosts that arrive in the same areas and thus may be the ultimate driver of mosquito-borne pathogen spread from sylvatic foci or endemic areas. Sequential spread or extreme events may extend the migrations into subtropical, Mediterranean, and even low latitude temperate zones, where susceptible populations are concentrated. Collectively, these features position wind-borne mosquito migration as an important, yet underappreciated mechanism for pathogen redistribution, bridging fragmented foci and ecosystems, sustaining transmission cycles, and reshaping the landscape of vector-borne disease risk. Public health decisions about risk of mid- and long-range mosquito-borne disease spread may consider susceptible populations downwind from active sources located up to hundreds of kilometers away and consider strategies to minimize emigration from active mosquito-borne disease transmission sources, monitoring along predominant wind "corridors," and readying rapid-response to abate local spread following indications of disease transmission in new destinations.

Materials and Methods

Study Sites. Aerial collection stations were established in Mali and Ghana: the Sahelian village, Thierola (13.659, −7.215, Mali), the Sudano-savanna village, Kenieroba (12.112, −8.332, Mali), the Guinea-savanna village, Bia (10.492, −5.910, Mali), the Guinea woodland ecozone near the town of Wenchi (7.781, −2.162, Ghana), and a moist-semi-deciduous forest near the town of Agogo (6.961, −0.960, Ghana). Locations for aerial sampling were selected rather arbitrarily based on position at a flat or rolling landscape, away from high topographic features, >10 km away from airports, and having a clearing ~500 m away from human houses, power lines, roads, and tall trees (3, 25, 27). No information on mosquito density or pathogen transmission was considered. Malian ecozones receive annual precipitation of 500 to 900 mm during the short-wet season (June–October), whereas in Ghana, annual precipitation varies between 1,200 and 1,500 mm and spreads during most months of the year (73). These study areas have been described previously (25, 58, 74), as have the field methods used in this study (3, 16, 25). Collections were made between March 2018 and October 2022. Due to logistical reasons, sampling intensity differed between localities with 50, 16, 67, 26, and 32 sampling nights in Thierola, Kenieroba, Bia, Wenchi, and Agogo, respectively.

Aerial Collection. The methods have been described in detail previously (3, 16, 25). Briefly, insect sampling was conducted using sticky nets (1 × 3 m panels) attached to the tethering line of helium-filled balloon (3 or 3.3 m diameter), with each balloon typically carrying three panels, suspended at 120, 160, and190 m agl on the 3 m balloon and 120, 190, 240, and 290 m agl on the 3.3 m balloon. Balloons were launched approximately 1 h before sunset and retrieved 1 h after sunrise, the following morning. To control for insects trapped near the ground as the panels were raised and lowered, comparable control panels were raised up to 100 m agl and immediately retrieved during each balloon launch and retrieval. Following panel retrieval, inspection for mosquitoes was typically carried out immediately, and specimens removed from the nets with forceps were briefly washed in chloroform to remove the insect-glue and individually stored in RNAlater™ (Invitrogen, Thermo Fisher Scientific, US). After several days in room temperatures in field conditions, specimens were placed in −20 °C freezers. Other insects were stored in vials containing 80% ethanol.

Specimen Processing and DNA/RNA Extraction. In the laboratory, mosquitoes were thawed on ice, placed momentarily on filter paper to absorb excess RNAlater™ solution, washed in deionized water and examined under dissecting microscope. Specimens were identified to genus or subfamily, their sex and gonotrophic state observed and recorded according to Sella scores: 1-2 for bloodfed, 3-5 for semigravid, and 6-7 for gravid (75). Initially, DNA/RNA extraction was carried on whole specimens. Later, the female's abdomen was dissected from her thorax, and each part was independently subjected to nucleic acid extraction as were whole bodies of male mosquitoes. Extractions following standard protocols are described in *SI Appendix*, Supplementary Results and Discussion. To preserve both RNA and DNA, no DNAses were added at the last steps of the extraction.

Mosquito Identification and Pathogen Screening. The mosquito mitochondrial *cytochrome oxidase I* (*COI*) gene was PCR amplified (76) using barcoded primers (identifying each amplicon) using 1.5 µL of the nucleic acids extracts (above). The 658-bp amplicons were sequenced using the Oxford Nanopore Technologies long-read MinION NGS platform, following established protocols (77, 78). A small minority of the specimens were subjected to standard PCR followed by Sanger sequencing (Eurofins Genomics, USA) of their amplicons after purification using the QIAquick PCR Purification Kit (QIAgen, USA).

Samples consisting of RNA/DNA extractions of females were screened individually for pathogen groups including flaviviruses, alphaviruses, Haemosporida, and filariae using group-specific real-time PCR assays with primers (and associated probes, *SI Appendix*, Table S5). To detect infection with Haemosporida, mosquitoes were screened with Haemosporida qPCR targeting the *COI* following an established protocol (79). Positive samples, defined as having CT<36 (80) were subjected to nested PCR amplification targeting 477 bp and 799 bp of *cytochrome b* (*cyt b*) (81–83) (*SI Appendix*, Table S5). *Anopheles* mosquitoes were also screened for human *Plasmodium* spp. using the qPCR assays of Bass et al. (84).

To detect infection with filarial nematodes, mosquito samples were screened using qPCR targeting *28S rRNA gene* (85). Positive samples subjected to standard PCR of the *COI gene* were confirmed by visualizing amplicons on 2% agarose gel (85) and sequenced using Sanger sequencing (Eurofins Genomic, USA). Infection with arboviruses of the genera Orthoflavivirus (and Alphavirus) were screened in the abdomens and head–thorax portions of mosquitoes by RT-qPCR associated with a high-resolution melting curve (86) using one step mixes (GoTaq® 1-Step RT-qPCR System, Promega, US). Positive flaviviruses samples were subjected to a nested PCR on a 960 bp fragment of the NsP5 gene (87), and purified amplicons were sequenced by Sanger sequencing (Eurofins Genomics, MD US). A subset of 48 samples were sequenced using the ONT MinION platform (below).

All PCR and qPCR assays had at least one negative (molecular grade water) and one positive control per assay. *Plasmodium falciparum*, *Brugia malayi*/*Dirofilaria immitis*, dengue virus, and Eilat virus (*Alphavirus Eilat*) were used as positive controls for the pan- Haemosporida, pan-nematode, pan-flavivirus, and pan-alphavirus assays, respectively. Most positive specimens by qPCR/PCR were amplified and sequenced twice, often with alternate primers. Verifications were carried out in spaced wells. Repeated PCR and sequencing of the mtCOI using thorax-head and abdomen showed high agreement between sequences. None of the wild positives detected *P. falciparum*, *D. immitis*, or another pathogen present in our laboratory, corroborating that contamination was well controlled, except dengue, in which genetic divergence between the DNEV control and the field isolates was high (total of 53 substitutions in 952 bp fragment).

Metagenomics on Selected Positive Samples. Metagenomic analyses on 48 individual mosquito abdomens found to be positive for flaviviruses (N = 29) or *Plasmodium* spp. (N = 10) or filariae (N = 9) divided into two pools of 24 samples were carried out using the MinION nanopore platform in two separate flow cells following methods as described in Supplementary Text.

Bioinformatics and Phylogenetic Analysis. The mosquito *COI* amplicon sequences, generated using the MinION were analyzed through ONTbarcoder version 1.9 or 2.0. Sequences of individual mosquitoes (amplicon metagenomics consensus per individual) and pathogens obtained by Sanger sequencing were blasted against repositories in BOLD, GenBank (NCBI) and, unless otherwise specified, species identity was provisionally given if sequence similarity was ≥98% (in most cases, it was ≥99%). Neighbor-joining (NJ) phylogenetic trees were used to cluster the sequences derived here in comparison to best matches from corresponding databases. Mosquito taxa that did not fit these criteria were provisionally named (e.g., *Aedes mali* sp. 1, *Culex* MBI-61) based on their sequence (or subfamily), in cases where molecular amplification failed repeatedly.

Metagenomic sequence database-calling and demultiplexing was accomplished on the device with the MinKNOW operating software v21.11.7 (Oxford Nanopore Technologies). See Supplementary Text for details.

Phylogenetic relationships among *Plasmodium* partial *cytb* gene sequences (470 bp) obtained in this study and assignment into putative species was done by mapping clusters generated by the software Assemble Species by Automatic Partitioning (ASAP) (88) on a phylogenetic tree that combined these isolates with previously reported haemosporidian sequences as described in Supplementary Text.

Species-specific mosquito exposure to blood was estimated as the fraction of gravid, semigravid, and blood-fed females combined as opposed to unfed females. Species-specific and whole sample infection rates were estimated across mosquito specimens with data on a particular pathogen (e.g., DENV) and groups of pathogens (flaviviruses, or vertebrate pathogens). Overall mosquito infection rate was estimated based on detection of either flavivirus, *Plasmodium* spp., or nematodes in any part of a mosquito (data on alphaviruses were not used because sequencing failed to confirm infection detected by the qPCR assay). In calculating infection rates, super-infected mosquitoes (infected with >1 pathogens, or in both body parts), were considered as single positives for that pathogen or pathogen groups. Disseminated infections were calculated based on the thorax and head body part alone. Abdominal infection rates were estimated based on that body part alone.

Statistical Analysis. Heterogeneity among species was evaluated using the contingency table likelihood ratio chi-square test after pooling species with sample size <6. If the fraction of cells with expected counts <5 was greater than 20%, we used exact tests based on Monte Carlo simulation of 10,000 samples using Proc Freq (89). Weighted regression analysis (using sample size per species as weight) and local regression to assess trends between variables were calculated using Proc Reg and Proc Sgplot in SAS (89).

Aerial density was estimated using the panel density of the species divided by the total air volume that passed through that net that night (i.e., aerial density = panel density/volume of air sampled, and volume of air sampled = panel surface area × mean nightly wind speed × sampling duration). The panel surface area was 3 m^2. Wind-speed data were obtained from the atmospheric reanalyses of the global climate (ERA5). Hourly data consisting of the eastward and northward components (horizontal vectors) of the wind were available at 31-km surface resolution at 2 and 300 m agl (1,000 and 975 mbar pressure levels). Overnight records (19:00 through to 06:00) were averaged to calculate the nightly mean direction and mean wind speed over each African sampling station based on standard formulae using code written in Base SAS (89). Nightly collections reflecting duration panels were suspended at altitude from 18:00 to 08:00 the following day (14 h sampling duration/night). The intensity of migration was expressed as the expected number of migrants/species crossing a line of 1 km perpendicular to the wind direction at altitude, which reflects their direction of movement (1, 3, 28, 90). We used the mean wind speed at altitude during the migration season (4.5 m/s) and assumed that the mosquitoes fly in a layer depth of 200 m agl (3, 25). The nightly migration intensity was computed across the 4-mo flight season (in which most species were sampled), including sampling nights during which no migrants were captured). The corresponding annual index was estimated for a sector of 100 km following previous publications (3, 25).

Data, Materials, and Software Availability. All data used in this paper are publicly available as follows. Mosquito species identification, sexual and gonotrophic state composition, and infection status: *SI Appendix*, and as a dataset in repository Figshare (91). The mosquito species-diagnostic mtDNA COI sequences are also publicly available in the Figshare repository (91). Metadata and sequence data of mosquito-borne pathogens (and other microorganisms detected) are available in the Figshare repository (92).

ACKNOWLEDGMENTS. We thank Drs. Jose' Ribeiro, Thomas Wellems, Carolina Barillas-Mury, Jesus Valenzuela, Mrs. Fatoumata Bathily, and Mrs. Margery Sullivan for their kind, professional, and vital support and Drs. Alvaro Molina-Cruz and Fabiano Oliveira for their valuable guidance and assistance with metagenomics and molecular analyses. Thanks go to Ms. Mona Kafaie for assistance in laboratory work. Special thanks go to the residents of the villages Thierola, Kenieroba, Bia, Dukusen, and Wenchi for their cooperation and hospitality.

Author affiliations: [a]Division of Intramural Research, Laboratory of Malaria and Vector Research, National Institute of Allergy and Infectious Diseases, National Institutes of Health, Rockville, MD 20852; [b]Malaria Research and Training Center/Faculty of Medicine, Pharmacy and Odonto-Stomatology University of Sciences, Techniques and Technologies of Bamako, Bamako BP1805, Mali; [c]Department of Entomology, Smithsonian Institution, National Museum of Natural History, Washington, DC 20002; [d]Department of Medical Microbiology, University of Ghana Medical School, University of Ghana, Accra POB KB 52, Ghana; [e]Department of Animal Biology and Conservation Science, University of Ghana, Accra POB KB 52, Ghana; [f]Biotechnology and Nuclear Agriculture Research Institute, Ghana Atomic Energy Commission, Accra POB LG 80, Ghana; [g]Biology Department/Institute of Genomics and Evolutionary Medicine, Temple University, Philadelphia, PA 19122; [h]Department of Microbiology and Immunology, University of Texas Medical Branch, Galveston, TX 77555; [i]World Reference Center of Emerging Viruses and Arboviruses, University of Texas Medical Branch, Galveston, TX 77555; [j]Department of Entomology, College of Plant Protection, Nanjing Agricultural University, Nanjing 210095, People's Republic of China; [k]Centre for Ecology and Conservation, University of Exeter, Penryn TR10 9FE, Cornwall, United Kingdom; [l]Natural Resources Institute, University of Greenwich, Chatham ME4 4TB, United Kingdom; and [m]Rothamsted Research, Harpenden, Hertfordshire AL5 2JQ, United Kingdom

Author contributions: R.B., A.D., A.S.Y., Y.A.A., Y.-M.L., and T.L. designed research; R.B., A.D., A.S.Y., C.K., K.E., B.P.B., M.D., Z.L.S., S.D., A.R.M., C.M.O.-A., G.A.-B., C.M.P.-Z., B.J.K., R.F., and R.N. performed research; S.C.W., J.W.C., and D.R.R. contributed new reagents/analytic tools; R.B., K.E., B.P.B., B.J.K., M.A.P., A.A.E., Y.-M.L., and T.L. analyzed data; R.B. and T.L. drafted the paper with inputs from K.E., M.A.P., A.A.E., and Y.-M.L.; and R.B., A.D., A.S.Y., C.K., K.E., B.P.B., M.D., Z.L.S., S.D., Y.A.A., A.R.M., C.M.O.-A., G.A.-B., C.M.P.-Z., B.J.K., R.F., M.A.P., A.A.E., S.C.W., R.N., J.W.C., D.R.R., Y.-M.L., and T.L. discussed and revised the paper.

1. G. Hu *et al.*, Mass seasonal bioflows of high-flying insect migrants. *Science* **354**, 1584–1587 (2016).
2. D. R. Reynolds, J. W. Chapman, R. Harrington, The migration of insect vectors of plant and animal viruses. *Adv. Virus Res.* **67**, 453–517 (2006).
3. J. Florio *et al.*, Diversity, dynamics, direction, and magnitude of high-altitude migrating insects in the Sahel. *Sci. Rep.* **10**, 20523 (2020).
4. V. A. Drake, R. A. Farrow, The influence of atmospheric structure and motions on insect migration. *Annu. Rev. Entomol.* **33**, 183–210 (1988).
5. V. A. Drake, Z. H. Hao, H. K. Wang, Monitoring insect numbers and biodiversity with a vertical-beam entomological radar. *Philos. Trans. R. Soc. Lond. B Biol. Sci.* **379**, 20230117 (2024).
6. R. A. Farrow, J. E. Dowse, Method of using kites to carry tow nets in the upper air for sampling migrating insects and its application to radar entomology. *Bull. Entomol. Res.* **74**, 87–95 (1984).
7. H. Dingle, V. A. Drake, What is migration? *Bioscience* **57**, 113–121 (2007).
8. J. W. Chapman, D. R. Reynolds, K. Wilson, Long-range seasonal migration in insects: Mechanisms, evolutionary drivers and ecological consequences. *Ecol. Lett.* **18**, 287–302 (2015).
9. N. J. Beeton, A. Wilkins, A. Ickowicz, K. R. Hayes, G. R. Hosack, Spatial modelling for population replacement of mosquito vectors at continental scale. *PLoS Comput. Biol.* **18**, e1009526 (2022).
10. D. Eagles, P. J. Walker, M. P. Zalucki, P. A. Durr, Modelling spatio-temporal patterns of long-distance dispersal into northern Australia. *Prev. Vet. Med.* **110**, 312–322 (2013).
11. B. H. Kay, R. A. Farrow, Mosquito (Diptera: Culicidae) dispersal: Implications for the epidemiology of Japanese and Murray Valley encephalitis viruses in Australia. *J. Med. Entomol.* **37**, 797–801 (2000).
12. S. N. Surendran *et al.*, Anopheline bionomics, insecticide resistance and transnational dispersion in the context of controlling a possible recurrence of malaria transmission in Jaffna city in northern Sri Lanka. *Parasit. Vectors* **13**, 156 (2020).

13. L. Sedda, D. J. Rogers, The influence of the wind in the Schmallenberg virus outbreak in Europe. *Sci. Rep.* **3**, 3361 (2013).
14. T. Lehmann *et al.*, Urban malaria may be spreading via the wind-here's why that's important. *Proc. Natl. Acad. Sci. U.S.A.* **120**, e2301666120 (2023).
15. T. Lehmann *et al.*, The African mosquito-borne diseasosome: Geographical patterns, range expansion and future disease emergence. *Proc. R. Soc. B Biol. Sci.* **290**, 20231581 (2023).
16. Z. L. Sanogo *et al.*, The effects of high-altitude windborne migration on survival, oviposition, and blood-feeding of the African Malaria Mosquito, *Anopheles gambiae* s.l. (Diptera: Culicidae). *J. Med. Entomol.* 58, 343–349 (2021).
17. D. E. Pedgley, D. R. Reynolds, G. M. Tatchell, "Long-range insect migration in relation to climate and weather: Africa and Europe" in *Insect Migration: Tracking Resources through Space and Time*, V. A. Drake, A. G. Gatehouse, Eds. (Cambridge University Press, Cambridge, UK, 1995), pp. 3–29.
18. C. Garrett-Jones, A dispersion of mosquitoes by wind. *Nature* **165**, 285 (1950).
19. C. Garrett-Jones, The possibility of active long-distance migrations by *Anopheles pharoensis* Theobald. *Bull. World Health Organ.* **27**, 299–302 (1962).
20. J. G. Ming *et al.*, Autumn southward return migration of the mosquito *Culex tritaeniorhynchus* in China. *Med. Vet. Entomol.* **7**, 323–327 (1993).
21. R. F. Sellers, Eastern equine encephalitis in Quebec and Connecticut, 1972: Introduction by infected mosquitoes on the wind? *Can. J. Vet. Res.* **53**, 76–79 (1989).
22. R. F. Sellers, D. E. Pedgley, M. R. Tucker, Possible spread of African horse sickness on wind. *J. Hyg. Camb.* **79**, 279–298 (1977).
23. R. F. Sellers, D. E. Pedgley, M. R. Tucker, Rift Valley fever, Egypt 1977: Disease spread by windborne insect vectors? *Vet. Rec.* **110**, 73–77 (1982).
24. R. F. Sellers, Weather, host and vector—Their interplay in the spread of insect-borne animal virus diseases. *J. Hyg. Camb.* **85**, 65–102 (1980).
25. D. L. Huestis *et al.*, Windborne long-distance migration of malaria mosquitoes in the Sahel. *Nature* **574**, 404–408 (2019).
26. A. S. Yaro *et al.*, Diversity, composition, altitude, and seasonality of high-altitude windborne migrating mosquitoes in the Sahel: Implications for disease transmission. *Front. Epidemiol.* **2**, 1001782 (2022).
27. H. E. Atieli *et al.*, Wind-assisted high-altitude dispersal of mosquitoes and other insects in East Africa. *J. Med. Entomol.* **60**, 698–707 (2023).
28. V. A. Drake, D. R. Reynolds, *Radar Entomology: Observing Insect Flight and Migration* (CABI International, 2012).
29. F. Tandina *et al.*, Mosquitoes (Diptera: Culicidae) and mosquito-borne diseases in Mali, West Africa. *Parasit. Vectors* **11**, 467 (2018).
30. D. Diallo *et al.*, Biodiversity pattern of mosquitoes in southeastern Senegal, epidemiological implication in arbovirus and malaria transmission. *J. Med. Entomol.* **56**, 453–463 (2019).
31. M. Diallo *et al.*, Mosquito vectors of the 1998–1999 outbreak of Rift Valley fever and other arboviruses (Bagaza, Sanar, Wesselsbron and West Nile) in Mauritania and Senegal. *Med. Vet. Entomol.* **19**, 119–126 (2005).
32. M. T. Gillies, T. J. Wilkes, A study of age-composition of populations of *Anopheles gambiae* Giles and *A. funestus* Giles in north-eastern Tanzania. *Bull. Entomol. Res.* **56**, 237–262 (1965).
33. J. D. Charlwood, E. V. Tomas, A. Egyir-Yawson, A. A. Kampango, R. J. Pitts, Feeding frequency and survival of *Anopheles gambiae* in a rice-growing area in Ghana. *Med. Vet. Entomol.* **26**, 263–270 (2012).
34. S. Bensch, O. Hellgren, J. Pérez-Tris, MalAvi: A public database of malaria parasites and related haemosporidians in avian hosts based on mitochondrial cytochrome lineages. *Mol. Ecol. Resour.* **9**, 1353–1358 (2009).
35. C. Garrett-Jones, Migratory flight in anopheline mosquitoes in the Middle East. *Bull. Endem. Dis. (Baghdad)* **2**, 79–87 (1956).
36. P. A. Glick, "The distribution of insects, spiders and mites in the air" in *Technical Bulletin* (United States Department of Agriculture, Washington, D.C. 1939), p. 151.
37. D. R. Reynolds *et al.*, Atmospheric transport of mosquitoes in northeast India. *Med. Vet. Entomol.* **10**, 185–186 (1996).
38. R. Garms, The reinvasion of the onchocerciasis control programme area in the Volta River Basin by *Simulium damnosum* s.l. the involvement of the different cytospecies and epidemiological implications. *Ann. Soc. Belg. Med. Trop.* **61**, 193–198 (1981).
39. R. Garms, J. F. Walsh, J. B. Davies, Studies on the reinvasion of the Onchocerciasis Control Programme in the Volta River Basin by *Simulium damnosum* s.l. with emphasis on the south-western areas. *Tropenmed. Parasitol.* **30**, 345–362 (1979).
40. R. A. Cheke, F. M. Hawkes, M. Carnaghi, Short- and long-term dispersal by members of *Simulium damnosum* Complex (Diptera: Simuliideae), vectors of onchocerciasis: A review. *Insects* **15**, 606 (2024).
41. S. Lion, M. van Baalen, W. G. Wilson, The evolution of parasite manipulation of host dispersal. *Proc. R. Soc. B Biol. Sci.* **273**, 1063–1071 (2006).
42. X. Martini, M. Hoffmann, M. R. Coy, L. L. Stelinski, K. S. Pelz-Stelinski, Infection of an insect vector with a bacterial plant pathogen increases its propensity for dispersal. *PLoS One* **10**, e0129373 (2015).
43. R. Poulin, D. D. Dutra, Animal migrations and parasitism: Reciprocal effects within a unified framework. *Biol. Rev.* **96**, 1331–1348 (2021).
44. J. L. Hardy, "Susceptibility and Resistance of Vector Mosquitoes" in *The Arboviruses: Epidemiology and Ecology*, T. P. Monath, Ed. (CRC Pres, Boca Raton, FL, 1988), vol. 1, pp. 87–126.
45. P. R. Grimstad, S. L. Paulson, G. B. Craig Jr., Vector competence of *Aedes hendersoni* (Diptera: Culicidae) for La Crosse virus and evidence of a salivary-gland escape barrier. *J. Med. Entomol.* **22**, 447–453 (1985).
46. T. W. Scott, L. H. Lorenz, S. C. Weaver, Susceptibility of *Aedes albopictus* to infection with eastern equine encephalomyelitis virus. *J. Am. Mosq. Control Assoc.* **6**, 274–278 (1990).
47. F. Dao *et al.*, The prevalence of human *Plasmodium* species during peak transmission seasons from 2016 to 2021 in the rural commune of Ntjiba, Mali. *Trop. Med. Infect. Dis.* **8**, 438 (2023).
48. M. Heinemann *et al.*, High prevalence of asymptomatic malaria infections in adults, Ashanti Region, Ghana, 2018. *Malar. J.* **19**, 366 (2020).
49. S. X. W. Gwee, A. L. St John, G. C. Gray, J. X. Pang, Animals as potential reservoirs for dengue transmission: A systematic review. *One Health* **12**, 100216 (2021).
50. G. Eastwood, R. C. Sang, J. Lutomiah, P. Tunge, S. C. Weaver, Sylvatic mosquito diversity in Kenya-considering enzootic ecology of arboviruses in an era of deforestation. *Insects* **11**, 342 (2020).
51. J. Figuerola *et al.*, A one health view of the West Nile virus outbreak in Andalusia (Spain) in 2020. *Emerg. Microbes Infect.* **11**, 2570–2578 (2022).
52. L. Ericson, J. J. Burdon, W. J. Müller, Spatial and temporal dynamics of epidemics of the rust fungus on populations of its host. *J. Ecol.* **87**, 649–658 (1999).
53. K. C. Harding, M. Begon, A. Eriksson, B. Wennberg, Increased migration in host-pathogen metapopulations can cause host extinction. *J. Theor. Biol.* **298**, 1–7 (2012).
54. B. Kerr, C. Neuhauser, B. J. M. Bohannan, A. M. Dean, Local migration promotes competitive restraint in a host-pathogen "tragedy of the commons". *Nature* **442**, 75–78 (2006).
55. A. L. Laine, Spatial scale of local adaptation in a plant-pathogen metapopulation. *J. Evol. Biol.* **18**, 930–938 (2005).
56. S. A. Moon, L. W. Cohnstaedt, D. S. McVey, C. M. Scoglio, A spatio-temporal individual-based network framework for West Nile virus in the USA: Spreading pattern of West Nile virus. *PLoS Comput. Biol.* **15**, e1006875 (2019).
57. A. M. Kilpatrick *et al.*, Predicting pathogen introduction: West Nile virus spread to Galapagos. *Conserv. Biol.* **20**, 1224–1231 (2006).
58. R. Nartey *et al.*, Invasion and spread of the neotropical leafhopper *Curtara insularis* (Hemiptera, Cicadellidae) in Africa and North America and the role of high-altitude windborne migration in invasive insects. *Neobiota* **96**, 173–189 (2024).
59. C. R. Brown, V. A. O'Brien, Are wild birds important in the transport of arthropod-borne viruses? *Ornithol. Monogr.* **71**, 1–64 (2011).
60. D. A. Satterfield, T. S. Sillett, J. W. Chapman, S. Altizer, P. P. Marra, Seasonal insect migrations: Massive, influential, and overlooked. *Front. Ecol. Environ.* **18**, 335–344 (2020).
61. J. Huang *et al.*, Massive seasonal high-altitude migrations of nocturnal insects above the agricultural plains of East China. *Proc. Natl. Acad. Sci. U.S.A.* **121**, e2317646121 (2024).
62. J. Soghigian *et al.*, Phylogenomics reveals the history of host use in mosquitoes. *Nat. Commun.* **14**, 6252 (2023).
63. M. W. Service, The identification of blood-meals from culicine mosquitos from Northern Nigeria. *Bull. Entomol. Res.* **55**, 637–643 (1965).
64. A. J. Haddow, Y. Ssenkubuge, Studies on the biting habits of East African mosquitos in the genera *Uranotaenia*, *Ficalbia* and *Hodgesia*. *Bull. Entomol. Res.* **53**, 639–652 (1963).
65. J. Rooyen, F. Lalubin, O. Glaizot, P. Christe, Avian haemosporidian persistence and co-infection in great tits at the individual level. *Malar. J.* **12**, 40 (2013).
66. S. L. Graff *et al.*, Detection of two alphaviruses: Middelburg virus and Sindbis virus from enzootic amplification cycles in southwestern Uganda. *Front. Microbiol.* **15**, 1394661 (2024).
67. N. Ayhan *et al.*, Detection and isolation of Sindbis virus from field collected mosquitoes in Timimoun, Algeria. *Viruses* **14**, 894 (2022).
68. R. C. Wilkerson, Y.-M. Linton, D. Strickman, *Mosquitoes of the World* (Johns Hopkins University Press, Baltimore, MD, 2021), vol. 2.
69. R. E. Tedrow *et al.*, *Anopheles* mosquito surveillance in Madagascar reveals multiple blood feeding behavior and Plasmodium infection. *PLoS Negl. Trop. Dis.* **13**, e0007176 (2019).
70. D. R. Reynolds, J. R. Riley, Radar observations of concentrations of insects above a river in Mali, West-Africa. *Ecol. Entomol.* **4**, 161–174 (1979).
71. M. T. O'Mara, M. Wikelski, B. Kranstauber, D. K. N. Dechmann, Common noctules exploit low levels of the aerosphere. *R. Soc. Open Sci.* **6**, 181942 (2019).
72. L. R. Taylor, Mortality and viability of insect migrants high in the air. *Nature* **186**, 410–410 (1960).
73. A. Siebert, Hydroclimate extremes in Africa: Variability, observations and modeled projections. *Geogr. Compass* **8**, 351–367 (2014).
74. A. Dao *et al.*, Signatures of aestivation and migration in Sahelian malaria mosquito populations. *Nature* **516**, 387–390 (2014).
75. T. S. Detinova, "Age-grouping methods in Diptera of medical importance with special reference to some vectors of malaria" in *Monograph Series* (*World Health Organization Monograph Series No. 47*, Geneva, Switzerland, 1962), pp. 13–191.
76. O. Folmer, M. Black, W. Hoeh, R. Lutz, R. Vrijenhoek, DNA primers for amplification of mitochondrial cytochrome c oxidase subunit I from diverse metazoan invertebrates. *Mol. Mar. Biol. Biotechnol.* **3**, 294–299 (1994).
77. A. Srivathsan *et al.*, Rapid, large-scale species discovery in hyperdiverse taxa using 1D MinION sequencing. *BMC Biol.* **17**, 96 (2019).
78. A. Srivathsan, V. Feng, D. Suárez, B. Emerson, R. Meier, ONTbarcoder 2.0: Rapid species discovery and identification with real-time barcoding facilitated by Oxford Nanopore R10.4. *Cladistics* **40**, 192–203 (2024).
79. O. Mediannikov *et al.*, Common epidemiology of *Rickettsia felis* infection and malaria, Africa. *Emerg. Infect. Dis.* **19**, 1775–1783 (2013).
80. A. Z. Diarra *et al.*, Molecular and MALDI-TOF identification of ticks and tick-associated bacteria in Mali (Publication with Expression of Concern). *Plos Negl. Trop. Dis.* **11**, e0005762 (2017).
81. O. Hellgren, U. Ottosson, J. Waldenström, S. Bensch, Avian malaria in Africa: The contact zone of two transmission areas. *Ostrich* **78**, 318–318 (2007).
82. T. J. Templeton, E. Martinsen, M. Kaewthamasorn, O. Kaneko, The rediscovery of malaria parasites of ungulates. *Parasitology* **143**, 1501–1508 (2016).
83. S. L. Perkins, J. J. Schall, A molecular phylogeny of malarial parasites recovered from cytochrome b gene sequences. *J. Parasitol.* **88**, 972–978 (2002).
84. C. Bass *et al.*, PCR-based detection of *Plasmodium* in *Anopheles* mosquitoes: A comparison of a new high-throughput assay with existing methods. *Malar. J.* **7**, 177 (2008).
85. Y. Laidoudi *et al.*, Development of a multiplex qPCR-based approach for the diagnosis of *Dirofilaria immitis*, *D. repens*, and *Acanthocheilonema reconditum*. *Parasit. Vectors* **13**, 319 (2020).
86. A. Vina-Rodriguez *et al.*, A Novel Pan-Flavivirus detection and identification assay based on RT-qPCR and microarray. *Biomed. Res. Int.* **2017**, 4248756 (2017).
87. A. Vazquez *et al.*, Novel flaviviruses detected in different species of mosquitoes in Spain. *Vector Borne Zoonotic Dis.* **12**, 223–229 (2012).
88. N. Puillandre, S. Brouillet, G. Achaz, ASAP: Assemble species by automatic partitioning. *Mol. Ecol. Resour.* **21**, 609–620 (2021).
89. SAS Institute Inc., SAS software (Version 9.4, Cary, NC, 2019).
90. D. R. Reynolds, J. W. Chapman, A. J. A. Stewart, Windborne migration of Auchenorrhyncha (Hemiptera) over Britain. *Eur. J. Entomol.* **114**, 554–564 (2017).
91. R. Bamou *et al.*, Dataset of high-flying mosquitoes with infection status. Figshare. https://doi.org/10.6084/m9.figshare.30406399.v2. Deposited 23 October 2025.
92. R. Bamou *et al.*, Metadata and sequences of pathogens isolated from wind-borne mosquitoes collected in Ghana and Mali. Figshare. https://doi.org/10.6084/m9.figshare.30524207.v1. Deposited 4 November 2025.

Pathogens spread by high-flying windborne mosquitoes

Supplementary Information

Roland Bamou[1], Adama Dao[2], Alpha S. Yaro[2], Cedric Kouam[1], Koray Ergunay[3], Brian P. Bourke[3], Moussa Diallo[2], Zana L. Sanogo[2], Samake Djibril[2], Yaw A. Afrane[4], Abdul Rahim Mohammed[4,5], Christopher M. Owusu-Asenso[4], Gabriel Akosah-Brempong[4,6], Cosmos M. Pambit-Zong[4], Benjamin J. Krajacich[1], Roy Faiman[1], M. Andreina Pacheco[7], Ananias A. Escalante[7], Scott C. Weaver[8], Rita Nartey[1], Jason W. Chapman[9,10], Don R. Reynolds[11,12], Yvonne-Marie Linton[3] and Tovi Lehmann[1*]

[1] Laboratory of Malaria and Vector Research, NIAID, NIH. Rockville, MD, USA
[2] Malaria Research and Training Center (MRTC) / Faculty of Medicine, Pharmacy and Odonto-stomatology, Bamako, Mali
[3] Department of Entomology, Smithsonian Institution, National Museum of Natural History, Washington DC, USA
[4] Department of Medical Microbiology, University of Ghana Medical School, University of Ghana, Accra, Ghana.
[5] Department of Animal Biology and Conservation Science, University of Ghana, Accra, Ghana.
[6] Biotechnology and Nuclear Agriculture Research Institute, Ghana Atomic Energy Commission, Accra, Ghana.
[7] Biology Department/Institute of Genomics and Evolutionary Medicine (iGEM), Temple University, Philadelphia, PA, USA
[8] Department of Microbiology & Immunology and World Reference Center for Emerging Viruses and Arboviruses, University of Texas Medical Branch, Galveston, Texas, USA
[9] Department of Entomology, College of Plant Protection, Nanjing Agricultural University, Nanjing, P. R. China.
[10] Centre for Ecology and Conservation, University of Exeter, Penryn, Cornwall, UK
[11] Natural Resources Institute, University of Greenwich, Chatham, Kent, UK
[12] Rothamsted Research, Harpenden, Hertfordshire, UK

*** Correspondence: Tovi Lehmann (tlehmann@niaid.nih.gov)**

Supplementary Results and Discussion

In this study we included samples collected at five aerial stations across West Africa to address the question of infection of high-altitude windborne mosquitoes with pathogens. A total of 1,247 mosquitoes were collected on 432 standard panels (sticky nets) but no mosquito was collected on 301 control panels, demonstrating that mosquitoes were collected while actively migrating high above the ground. Larger numbers of female mosquitoes were sampled in Ghana (656; Agogo and Wenchi) than in Mali (361; Bia, Kenieroba, and Thierola, Fig. S1a). A species-specific comparison of the high-altitude mosquito and pathogen compositions among these sites requires a larger sample size from most sites. Overall, infection with mosquito-borne pathogens was similar across sites (Fig S1b) and no significant variation was detected (Likelihood Ratio Chi-Square=3.81, N=1008, df=4, P=0.43, Fig. S1b). Separate tests comparing infection rates of *Plasmodium*, filariae, and flaviviruses among localities, were also non-significant (P>0.05, Fig. S1b). Although a larger sample size may detect differences in infection rates among localities, these results suggest pathogen transport across ecozones are similar and raise the possibility of connectivity among them. High-altitude windborne migration in West African mosquitoes is evidently common, as it occurs in ≥34% (61/181) of the mosquito species given that the combined mosquito fauna in Mali (105 species) and Ghana (155 species) comprises 181 species (*1*). In this study, we describe, for the first time, the composition of mosquito-borne pathogens and their high-altitude mosquito carriers over Africa.

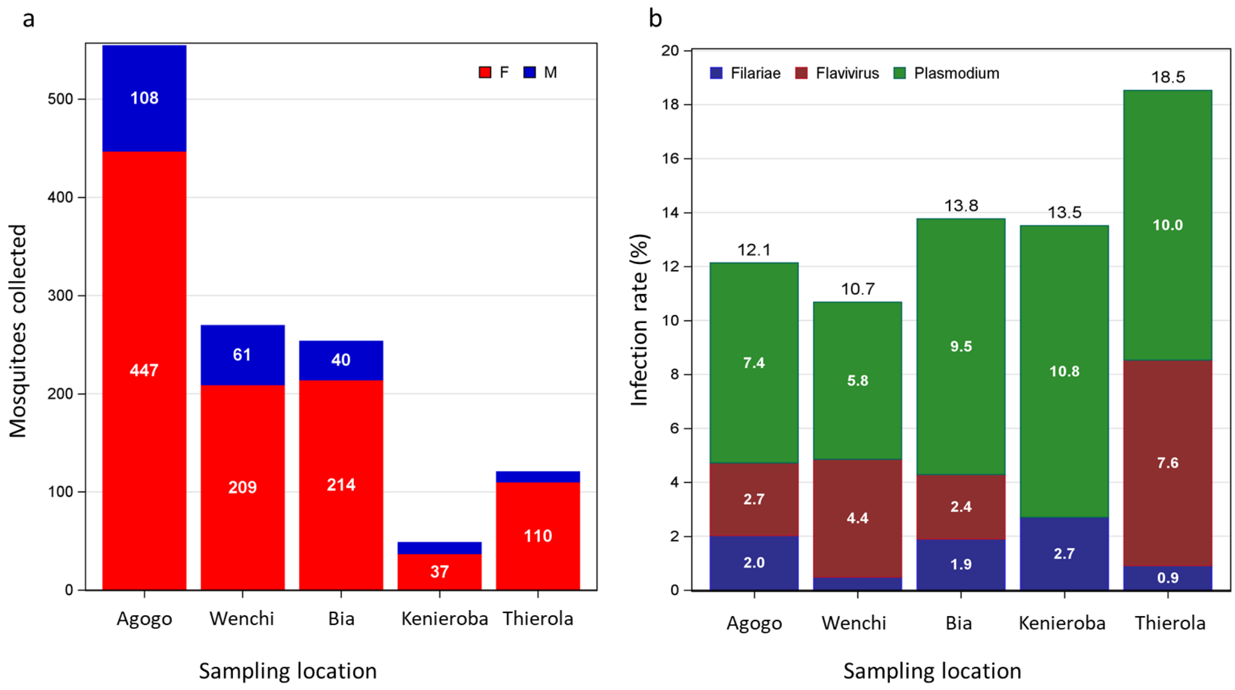

Figure S1. Sources of mosquitoes used in the present study among the aerial sampling stations by sex (a) and the overall rates of infection with the main pathogen groups (white, within bar segments) and overall (black, top) across aerial stations.

The composition distribution of high-flying mosquitoes (Fig. 1a, Table S1) is typical of biological samples in being dominated by a few common species whilst most are moderately abundant or rare (*2*). This distribution likely reflects the abundance of these species on the ground (over large catchment areas) and their propensity to engage in high-altitude windborne migration. Few of the rare species may represent incidental events, although most simply reflect low aerial density. *Aedes aegypti* may represent an incidental event, being a diurnal species that is attracted to people, and because it includes two mosquitoes collected on the same panel during first operation of a newly trained team. Additional studies will ascertain the status of rare species. The activity rhythms of most species reported here are not well known, but many diurnal insects, e.g., grasshoppers, Chrysomelid beetles, wasps, and blackflies migrate at altitude during nighttime (Drake and Reynolds 2012, Florio et al. 2020). Entomological radars in tropical regions consistently show higher insect densities at altitude during the night than during the day, and also a sharp increase of insect flight activity upwards around dusk, scaled 10-100x, climbing from surface to few hundred meters (*3*). Unless temperatures at altitude are <16°C (uncommon in tropical regions), most insect migration at altitude occurs at night.

Consistent with previous studies (*4-6*), at altitude female mosquitoes predominated (85%). This sex ratio held constant independent of species (P=0.063, Monte Carlo Exact Test for contingency tables, Table S2). Because females typically are inseminated by males from their site of origin, this asymmetry in long-range migration should not have consequences on sex-specific geneflow (*7*). The female bias likely reflects the sexual fitness differential associated with long-range migration. Accordingly, upon landing females need only find bodies of water suitable for larval development that typically abound after the first rains throughout the rainy season, whereas males need to locate virgin females. During the early phases of population growth, density is low, and females are scarce, consequently diminishing the expected mating success of migrant males. Even if populations are at their peak, male migrants must compete with local males that are produced in equal proportion to females—as in their provenance site (*8, 9*). Migration is expected to tax (*10*) the male's competitive ability, increasing the risk of failing to mate after landing. Although mating at an area with lower predation, parasitism, and competition is expected to increase male fitness too, the above costs reduce migrant male's expected benefit compared with that of female migrants. The hypothesis that feeding on birds increases a mosquito's likelihood to engage in high-altitude migration because of the lower abundance of hosts linked to bird migration, seems unlikely, but it cannot be ruled out, especially because it partly explains the female predominance and possibly the seasonality of mosquito migration.

Heterogeneity in the fraction of gravid and unfed females has been detected among species (Table S3). Because all gravid females have had at least one exposure to vertebrate blood whereas some of the unfed females may have departed prior to their first blood-feeding, it is expected that infection rate in gravid females will be higher than in unfed females. Pooling the blood-fed (N=6) and the semi-gravid females (N=10) with gravid females (N=414) and contrasting them with the unfed females (N=545) revealed a higher infection rate (across pathogen groups) in gravid compared with unfed females (18.4% vs. 8.8%, P<0.0001, Fisher Exact Test). This difference was driven by infection with *Plasmodium* spp. (12.6% vs. 4.8%, P<0.0001, Fisher Exact Test) but the trend held for flaviviruses (4.2% vs. 2.8%, P=0.22, Fisher Exact Test) and filariae (2.1% vs. 1.3%, P=0.23, Fisher Exact Test). Considering species with sample size >10, the proportion of gravid females per species did not predict its overall infection rate in a regression analysis (N=12, $F_{1/10}$=2.83, P=0.12 r^2= 0.22). Nonetheless, widespread infection with vertebrate pathogens in unfed females implies that at least a fraction of them have taken one or more blood meals from vertebrate hosts prior to their journey and supports a migration strategy involving older females. The ratio of the rates of infectiousness (i.e., disseminated infection) over exposure ("infected"; inclusive for all body parts) in a sample of mosquitoes can be used to estimate the fraction of mosquitoes above the minimum age, required to develop a disseminated infection (*11, 12*). In tropical areas, *Plasmodium* spp. typically require ≥7 days post infection to mature their oocysts in the midgut wall (abdomen) and release sporozoites into the haemocoel that accumulate in the salivary glands (thorax), thus initiating a disseminated infection. The first blood meal typically takes place on the adult's second day (*11-13*). This ratio across all *Plasmodium* species with at least one disseminated infection (to indicate that the mosquito species can support the parasite), was 0.5 (0.031/0.062; Table 1), implying that half the population is ≥9 days old. This high rate indicates an older age distribution, which is 2.5 times the typical fraction of mosquitoes of this age class (that had taken ≥3 bloodmeals on vertebrate hosts (*12*)), thus explaining, at least in part, the high infection rates in this collection. Whether pathogens increase the aptitude of infected mosquitoes to engage in high-altitude windborne migration (*14-16*) remains to be answered. The high proportion of gravid and older females (*6*), supports that migration is a bet-hedging evolved behavior by embarking on migration when females are ready to lay eggs, unencumbered by requirements of localizing a mate, a host, etc., and probably after completing at least one oviposition cycle at their area of origin.

With 15 putative *Plasmodium* species detected in this sample of high-flying mosquitoes being a conservative estimate, given the grouping of genotypes implemented by ASAP, and the discovery of four previously undescribed putative species (Methods, Fig. S2), the diversity of *Plasmodium* species is remarkably high.

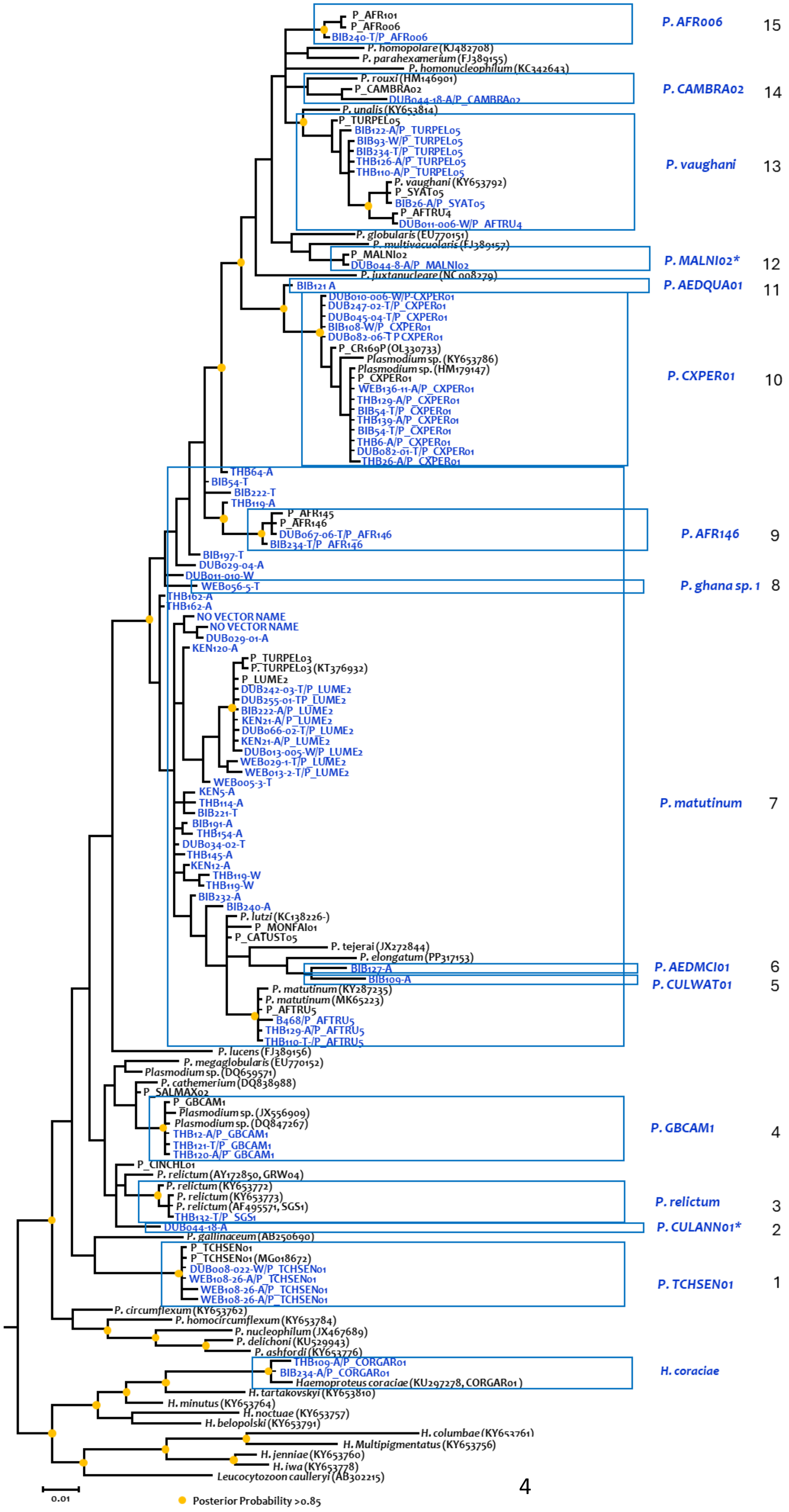
P_AFR101
P_AFR006
BIB240-T/P_AFR006
P. AFR006
15
P. homopolare (KJ482708)
P. parahexamerium (FJ389155)
P. homonucleophilum (KC342643)
P. rouxi (HM146901)
P_CAMBRA02
DUB044-18-A/P_CAMBRA02
P. CAMBRA02
14
P. unalis (KY653814)
P_TURPEL05
BIB122-A/P_TURPEL05
BIB93-W/P_TURPEL05
BIB234-T/P_TURPEL05
THB126-A/P_TURPEL05
THB110-A/P_TURPEL05
P. vaughani (KY653792)
P_SYAT05
BIB26-A/P_SYAT05
P_AFTRU4
DUB011-006-W/P_AFTRU4
P. vaughani
13
P. globularis (EU770151)
P. multivacuolaris (FJ389157)
P_MALNI02
DUB044-8-A/P_MALNI02
P. MALNI02*
12
P. juxtanucleare (NC 008279)
BIB121 A
P. AEDQUA01
11
DUB010-006-W/P_CXPER01
DUB247-02-T/P_CXPER01
DUB045-04-T/P_CXPER01
BIB108-W/P_CXPER01
DUB082-06-T P CXPER01
P_CR169P (OL330733)
Plasmodium sp. (KY653786)
Plasmodium sp. (HM179147)
P_CXPER01
WEB136-11-A/P_CXPER01
THB129-A/P_CXPER01
BIB54-T/P_CXPER01
THB139-A/P_CXPER01
BIB54-T/P_CXPER01
THB6-A/P_CXPER01
DUB082-01-T/P_CXPER01
THB26-A/P_CXPER01
P. CXPER01
10
THB64-A
BIB54-T
BIB222-T
THB119-A
P_AFR145
P_AFR146
DUB067-06-T/P_AFR146
BIB234-T/P_AFR146
P. AFR146
9
BIB197-T
DUB029-04-A
DUB011-010-W
WEB056-5-T
P. ghana sp. 1
8
THB162-A
THB162-A
NO VECTOR NAME
NO VECTOR NAME
DUB029-01-A
KEN120-A
P_TURPEL03
P. TURPEL03 (KT376932)
P_LUME2
DUB242-03-T/P_LUME2
DUB255-01-TP_LUME2
BIB222-A/P_LUME2
KEN21-A/P_LUME2
DUB066-02-T/P_LUME2
KEN21-A/P_LUME2
DUB013-005-W/P_LUME2
WEB029-1-T/P_LUME2
WEB013-2-T/P_LUME2
WEB005-3-T
KEN5-A
THB114-A
BIB221-T
BIB191-A
THB154-A
DUB034-02-T
THB145-A
KEN12-A
THB119-W
THB119-W
BIB232-A
BIB240-A
P. lutzi (KC138226-)
P_MONFAI01
P_CATUST05
P. tejerai (JX272844)
P. elongatum (PP317153)
BIB127-A
BIB109-A
P. matutinum (KY287235)
P. matutinum (MK65223)
P_AFTRU5
B468/P_AFTRU5
THB129-A/P_AFTRU5
THB110-T-/P_AFTRU5
P. matutinum
7
P. AEDMCI01
6
P. CULWAT01
5
P. lucens (FJ389156)
P. megaglobularis (EU770152)
Plasmodium sp. (DQ659571)
P. cathemerium (DQ838988)
P_SALMAX02
P_GBCAM1
Plasmodium sp. (JX556909)
Plasmodium sp. (DQ847267)
THB12-A/P_GBCAM1
THB121-T/P_GBCAM1
THB120-A/P_GBCAM1
P. GBCAM1
4
P_CINCHL01
P. relictum (AY172850, GRW04)
P. relictum (KY653772)
P. relictum (KY653773)
P. relictum (AF495571, SGS1)
THB132-T/P_SGS1
P. relictum
3
DUB044-18-A
P. CULANN01*
2
P. gallinaceum (AB250690)
P_TCHSEN01
P_TCHSEN01 (MG018672)
DUB008-022-W/P_TCHSEN01
WEB108-26-A/P_TCHSEN01
WEB108-26-A/P_TCHSEN01
WEB108-26-A/P_TCHSEN01
P. TCHSEN01
1
P. circumflexum (KY653762)
P. homocircumflexum (KY653784)
P. nucleophilum (JX467689)
P. delichoni (KU529943)
P. ashfordi (KY653776)
THB109-A/P_CORGAR01
BIB234-A/P_CORGAR01
Haemoproteus coraciae (KU297278, CORGAR01)
H. coraciae
H. tartakovskyi (KY653810)
H. minutus (KY653764)
H. noctuae (KY653757)
H. belopolski (KY653791)
H. columbae (KY653761)
H. Multipigmentatus (KY653756)
H. jenniae (KY653760)
H. iwa (KY653778)
Leucocytozoon caulleryi (AB302215)
0.01
● Posterior Probability >0.85

Figure S2. Bayesian phylogeny of *Plasmodium* and *Haemoproteus* taxa isolated from high-altitude mosquitoes based on their mitochondrial *cytb* gene (blue font) including best-match sequences from MalAvi and NCBI databases (black) superimposed with species delimitation grouping using Assemble Species by Automatic Partitioning (ASAP, numbered squares). Posterior probabilities >0.85 signifying supported clades are shown using a yellow dot. A conservative ASAP grouping (fewest putative species) reflects ≤1.5% sequence dissimilarity and 15 putative species (squares) that were provisionally named after the closest species or lineage found in MalAvi that were grouped together. Groups that had no such match were named using the first 3 letters of the genus and species of their mosquito-host (MalAvi convention), unless unknown, when the country of collection was used, e.g., *P. Ghana sp. 1*. Samples with apparent mixed infection, which may result in chimeric sequences were indicated with '*'. *Haemoproteus coraciae* is a species of a closely related genus that is vectored by non-mosquito biting flies.

This diversity reflects sampling across ecozones from the Sahel to the equatorial forest (Methods), enhanced by the large catchment area of the aerial stations (tens to hundreds of kilometer radius around each station, Discussion). These results are not specific to *Plasmodium* as they also apply to the Culicidae (Fig. 1a) and to pathogens in general (Tables 1 and S4). Additionally, aerial collections provide information on movement trajectories, putative sources, and destinations of pathogens and vectors. High throughput aerial sampling methods, such as long-flying drones need be developed to facilitate pragmatic surveillance applications.

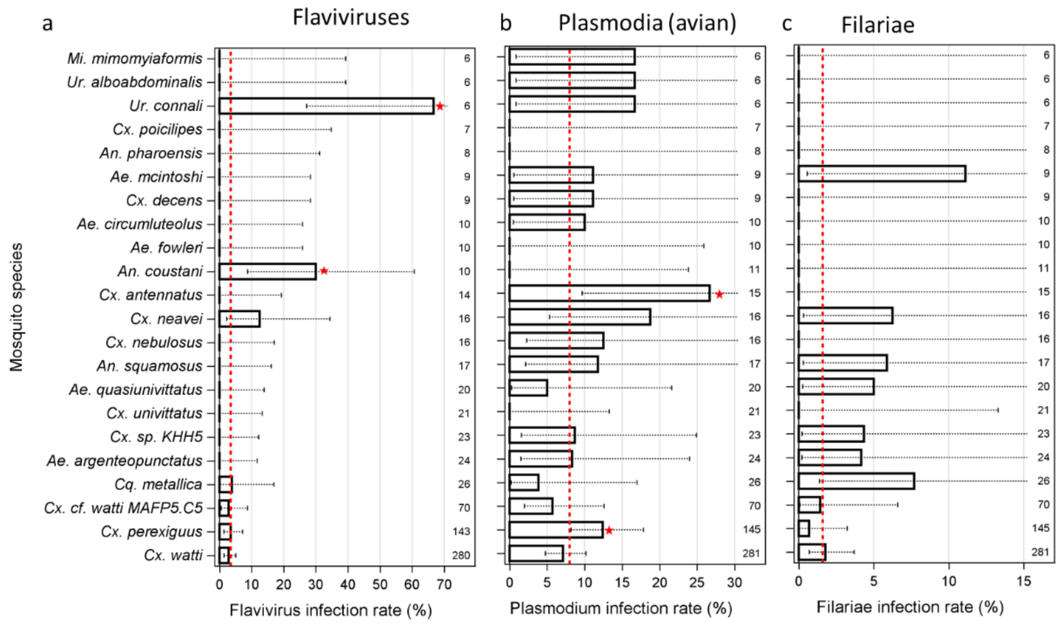

Figure S3. Overall infection rates per mosquito species (N>5) for flaviviruses (a), *Plasmodium* spp. (b), and filariae (c) with 90% CI. Higher infection rate (P<0.05, one-side Monte Carlo Exact Test for contingency tables) than the rate across all mosquito species (3.5%, 8%, and 1.6% for flaviviruses, *Plasmodium* spp., and filariae, respectively; red lines) are indicated by stars.

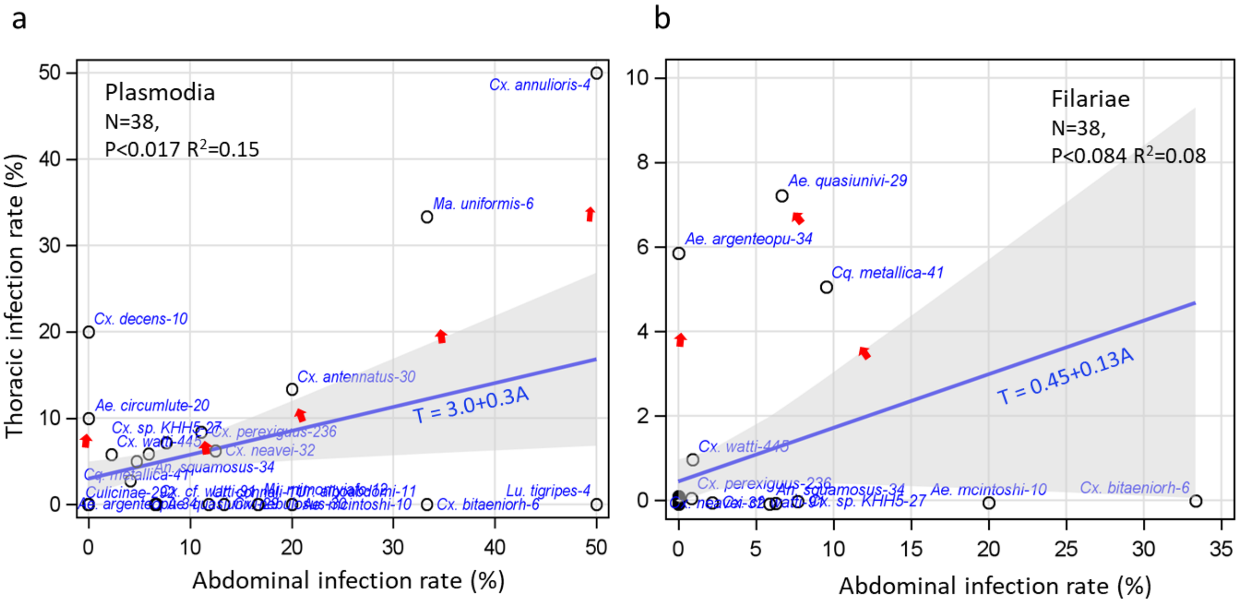

Figure S4. Relationship between disseminated (head-thorax) infection and exposure (abdominal) infection with *Plasmodium* spp. (a) and filariae (b) by species (abbreviated species name is listed with their sample size for infected species). Weighted linear regression (weighted by total sample size, blue) and 95% CI (gray) computed for species with N≥3 to identify outliers (red arrows) indicating competent vectors that selectively feed on natural hosts, showing increased exposure.

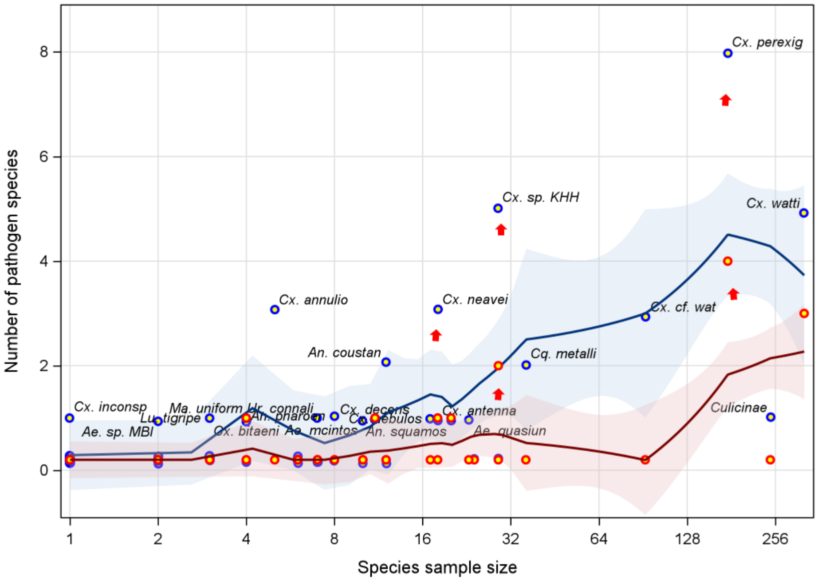

Figure S5. Effect of the species sample size on the number of pathogen species for which it is infected and infectious. Local regression (loess) lines with 95% CI describe the change in the number of pathogens species per mosquito species according to its ample size (log scale). Disseminated (head-thorax) infection (red) and total infection (blue) are shown. Abbreviated species name is listed for species with one or more pathogen species (black) and red arrows indicate infected and infectious species with elevated number of pathogens, respectively.

The long-range windborne migration of mosquitoes at altitude and their spread of pathogens has gone mostly unnoticed by entomologists and epidemiologists not only because this movement escapes direct observation. More importantly are the omnipresence of people and domestic animals and their extensive mobility that lend support to the argument that human movement or transport is the driver of pathogen spread in nearly all cases regardless of whether this is true. Therefore, proposing long-range windborne-mosquito-driven spread of pathogens requires extremely stringent conditions: i) outbreaks must occur outside the “endemic disease range”, which may be diffuse and patchy; ii) outbreaks should occur beyond a barrier that absolutely prevents vertebrate-host movement; and iii) data on wind direction and speed are available and closely align with the nearest known source of the disease (and the vector), during a narrow time window (typically of few days) during which the first case(s) were detected (*17-23*). There is often lack of knowledge about the time window of vector arrival and the presence of additional sources of the infected insects, especially when analysis pertained to zoonotic pathogens circulating in sylvatic cycles that remain mostly unknown (*1*). These requirements have restricted the number of “proven” cases, supporting the view that these are rare accidental events. We hope that the present study will encourage a greater attention to this modality of pathogen spread, its underlying drivers, and its implications.

Supplementary Methods

Extractions of nucleic acids were carried out using Trizol (TRI Reagent®, Zymo Research, US) after tissue homogenization using low-bind beads (in a Mini-BeadBeater-96 (BioSpec Products, Inc., Bartlesville, OK, USA) at a max speed for 30 s, repeated three times with 30 sec intermissions to dissipate heat. This slurry was spun at 13,000 g at 4ºC for 5 min to clear solids, and the supernatant was used for the extraction using Mag-Bind® Viral DNA/RNA 96 Kit (Zymo Research, US) using the KingFisher® Flex auto-extraction robot (ThermoFisher, US). The extracted nucleic acids were suspended in 50 µl of molecular grade water.

Metagenomic analyses on 48 individual mosquito abdomens found to be positive for flaviviruses (N=29) or *Plasmodium* spp. (N=10) or filariae (N=9) divided into two pools of 24 samples were carried out using MinION nanopore platform in two separate flow cells following methods as previously described(*24*). Briefly, the cDNA library was prepared as previously described (*25*). Using the RevertAid First Strand cDNA Synthesis Kit (Thermo Fisher Scientific), purified nucleic acids were converted to complementary DNA (cDNA) while random primer mix (New England Biolabs, Ipswich, MA, USA) was used to prepare double-stranded cDNA using NEBNext Non-Directional RNA Second Strand Synthesis module. Barcoded cDNA with the Native Barcoding Expansion 96-EXP-NBD 196 (Oxford Nanopore Technologies, Oxford, UK) was synthesized using automatic device, epiMotion 5075 (Eppendorf, US). Double stranded cDNA was cleaned up using Agencourt AMPure XP reagent (Beckman Coulter Biosciences, Indianapolis, IN, USA) and quantitated by Qubit dsDNA HS Assay Kit (ThermoFisher Scientific, Waltham, MA, USA). The NEBNext Ultra II End repair/dA-tailing and Quick Ligation modules (New England Biolabs, Ipswich, MA, USA), and Ligation Sequencing Kit SQK-LSK114 (Oxford Nanopore Technologies, Oxford, UK) were used to prepare libraries, which were further quantitated by Qubit (ThermoFisher Scientific, Waltham, MA, USA) using 1 × dsDNA HS Assay Kit. Metagenomic sequencing was accomplished using one pool (24 samples) per flow cell (Flow Cell

(R10.4.1), and run on the MinION or GridION sequencing device (Oxford Nanopore Technologies, Oxford, UK) for 72 h.

Metagenomic sequence raw reads generated using Oxford Nanopore Technologies and Guppy v5.1.13 (*26*) were trimmed with Porechop(*27*) to remove adapter sequences and then filtered with NanoFilt (*28*) to remove reads with q-scores ≤ 9 and read lengths ≤100bp. Reads from mosquito hosts were mapped to mosquito RefSeq refence genomes from the three main genera encountered (Aedes aegypti, GCF_002204515.2; Anopheles gambiae, GCF_000005575.2; Culex pipiens, GCF_016801865.2) using Minimap2 v2.24 (*29*) and removed using Samtools v1.9 (*30*). The resulting data was then used as input for metagenomic assembly using the Geneious Prime v2023.2.1 (Biomatters Ltd., Auckland, New Zealand) de novo assembly tool. Both reads and de novo assembled contigs were separately aligned to the National Center for Biotechnology Information (NCBI) protein non-redundant (nr) database (http://ftp.ncbi.nlm.nih.gov/blast/db/FASTA/nr.gz) using Diamond (--long-reads; --evalue 1e-6) (Buchfink et al., 2015, 2021) and taxonomically classified using Megan v6.24.20 (--minSupport 1; --minPercentIdentity 70; --maxExpected 1.0E-6; --lcaAlgorithm longReads; --lcaCoveragePercent 51; −-longReads) (*31*). Reads and contigs of taxonomic importance were further mapped to reference genomes within Geneious Prime using Minimap2 presets -x map-ont (mapping noisy reads of up to 10% error rate) and -x asm20 (contigs of up to 20% divergence), respectively. BLASTn and BLASTp searches were used to identify the most similar records in the NCBI database. The clustal algorithm (*32*) in Seaview (*33*) was used for sequence alignment and pairwise comparisons.

Phylogenetic relationships among *Plasmodium* partial *cytb* gene sequences (470 bp) obtained in this study and previously reported haemosporidian sequences were estimated on an alignment performed using ClustalX v2.0.12 and Muscle as implemented in SeaView v4.3.5 (*33*) with manual editing. Phylogenetic hypotheses were assessed based on this alignment using a Bayesian method implemented in MrBayes v3.2.7 with the default priors (*34*), and a general time-reversible model with gamma-distributed substitution rates, and a proportion of invariant sites (GTR + Γ + I) as it was the best model that fit the data with the lowest Bayesian information criterion scores estimated by MEGA v7.0.26 (*35*). Bayesian supports were inferred for the nodes in MrBayes by sampling every 1000 generations from 2 independent chains lasting 2×10^6 Markov Chain Monte Carlo steps. The chains were assumed to have converged once the potential scale reduction factor value was between 1.00 and 1.02, and the average standard deviation of the posterior probability was <0.01. 25% of the samples were discarded as a ‘burn-in’ once convergence was reached. Lineages names of all sequences (partial *cytb* gene) used here are shown in the phylogenetic trees and new isolates were named after their mosquito identification code. The phylogenetic tree of the *Plasmodium* isolates was used to confirm species assignment by comparison to sequences of taxa included in the MalAvi (*36*) and NCBI databases. The latter comprised of 40 published sequences including *P. matutinum*, *P. vaughani*, *P. relictum*, *P. cathemerium* as well as the closely related sister taxa *Haemoproteus coraciae* and *Leucocytozoon* sp. as outgroups to root and stabilize the tree topology (Fig. S2). *Plasmodium* taxa that mapped >3% sequence divergence from their nearest neighbor and away from their named best match were provisionally named *P. mali* sp. 1, etc. To resolve boundaries between certain clusters we used the software Assemble Species by Automatic Partitioning (ASAP) (*37*) using sequences generated in this project with closely matched taxa from MalAvi (plasmodia) or BOLD (mosquitoes) and selecting among the most conservative classifications supported.

References (including for the Supplementary Information)

1. T. Lehmann *et al.*, The African mosquito-borne diseasosome: geographical patterns, range expansion and future disease emergence. *P Roy Soc B-Biol Sci* **290**, 20231581 (2023).
2. H. G. Anderwartha, L. C. Birch, *The Distribution and Abundance of Animals*. (The University of Chicago Press, Chicago, 1954).
3. V. A. Drake, D. R. Reynolds, *Radar Entomology: Observing Insect Flight and Migration*. (CABI International, 2012).
4. H. E. Atieli *et al.*, Wind-assisted high-altitude dispersal of mosquitoes and other insects in East Africa. *J Med Entomol* **60**, 698–707 (2023).
5. D. L. Huestis *et al.*, Windborne long-distance migration of malaria mosquitoes in the Sahel. *Nature* **574**, 404–408 (2019).
6. A. S. Yaro *et al.*, Diversity, composition, altitude, and seasonality of high-altitude windborne migrating mosquitoes in the Sahel: Implications for disease transmission. *Frontiers in Epidemiology* **13 October 2022**, (2022).
7. M. B. Barth, R. F. A. Moritz, C. W. W. Pirk, F. B. Kraus, Male-biased dispersal promotes large scale gene flow in a subterranean army ant, *Dorylus (Typhlopone) fulvus*. *Popul Ecol* **55**, 523–533 (2013).
8. A. Diabaté *et al.*, Spatial distribution and male mating success of *Anopheles gambiae* swarms. *Bmc Evol Biol* **11**, (2011).
9. K. R. Dabire *et al.*, Assortative mating in mixed swarms of the mosquito *Anopheles gambiae* s.s. M and S molecular forms, in Burkina Faso, West Africa. *Medical and Veterinary Entomology* **27**, 298–312 (2013).
10. H. Dingle, V. A. Drake, What is migration? *Bioscience* **57**, 113–121 (2007).
11. M. T. Gillies, The Recognition of Age-Groups within Populations of Anopheles-Gambiae by the Pre-Gravid Rate and the Sporozoite Rate. *Ann Trop Med Parasit* **48**, 58–74 (1954).
12. M. T. Gillies, T. J. Wilkes, A Study of Age-Composition of Populations of Anopheles Gambiae Giles and a Funestus Giles in North-Eastern Tanzania. *B Entomol Res* **56**, 237–+ (1965).
13. M. T. Gillies, T. J. Wilkes, Observations on Nulliparous and Parous Rates in a Population of Anopheles Funestus in East Africa. *Ann Trop Med Parasit* **57**, 204–& (1963).
14. S. Lion, M. van Baalen, W. G. Wilson, The evolution of parasite manipulation of host dispersal. *P Roy Soc B-Biol Sci* **273**, 1063–1071 (2006).
15. X. Martini, M. Hoffmann, M. R. Coy, L. L. Stelinski, K. S. Pelz-Stelinski, Infection of an Insect Vector with a Bacterial Plant Pathogen Increases Its Propensity for Dispersal. *Plos One* **10**, (2015).
16. R. Poulin, D. D. Dutra, Animal migrations and parasitism: reciprocal effects within a unified framework. *Biol Rev* **96**, 1331–1348 (2021).
17. C. Garrett-Jones, A dispersion of mosquitoes by wind. *Nature* **165**, 285 (1950).
18. C. Garrett-Jones, Migratory flight in anopheline mosquitoes in the Middle East. *Bull Endem Dis (Baghdad)* **2**, 79–87 (1956).
19. C. Garrett-Jones, The possibility of active long-distance migrations by Anopheles pharoensis Theobald. *Bull World Health Organ* **27**, 299–302 (1962).
20. D. E. Pedgley, Windborne Spread of Insect-Transmitted Diseases of Animals and Man. *Philos T R Soc B* **302**, 463–470 (1983).
21. R. F. Sellers, A. R. Maarouf, Trajectory analysis of winds and eastern equine encephalitis in USA, 1980-5. *Epidemiol Infect* **104**, 329–343 (1990).
22. R. F. Sellers, D. E. Pedgley, M. R. Tucker, Possible Spread of African Horse Sickness on Wind. *J Hyg-Cambridge* **79**, 279–298 (1977).

23. R. F. Sellers, D. E. Pedgley, M. R. Tucker, Rift Valley fever, Egypt 1977: disease spread by windborne insect vectors? *Vet Rec* **110**, 73–77 (1982).
24. K. Ergunay *et al.*, The expanding range of emerging tick-borne viruses in Eastern Europe and the Black Sea Region. *Sci Rep* **13**, 19824 (2023).
25. J. Kamau *et al.*, A Novel Coronavirus and a Broad Range of Viruses in Kenyan Cave Bats. *Viruses* **14**, (2022).
26. R. R. Wick, L. M. Judd, K. E. Holt, Performance of neural network basecalling tools for Oxford Nanopore sequencing. *Genome Biol* **20**, (2019).
27. R. R. Wick, L. M. Judd, C. L. Gorrie, K. E. Holt, Completing bacterial genome assemblies with multiplex MinION sequencing. *Microb Genomics* **3**, (2017).
28. W. De Coster, S. D'Hert, D. T. Schultz, M. Cruts, C. Van Broeckhoven, NanoPack: visualizing and processing long-read sequencing data. *Bioinformatics* **34**, 2666–2669 (2018).
29. H. Li, Minimap2: pairwise alignment for nucleotide sequences. *Bioinformatics* **34**, 3094–3100 (2018).
30. P. Danecek *et al.*, Twelve years of SAMtools and BCFtools. *Gigascience* **10**, (2021).
31. C. Bagci, S. Patz, D. H. Huson, DIAMOND plus MEGAN: Fast and Easy Taxonomic and Functional Analysis of Short and Long Microbiome Sequences. *Curr Protoc* **1**, (2021).
32. F. Sievers, D. G. Higgins, Clustal Omega for making accurate alignments of many protein sequences. *Protein Sci* **27**, 135–145 (2018).
33. M. Gouy, S. Guindon, O. Gascuel, SeaView Version 4: A Multiplatform Graphical User Interface for Sequence Alignment and Phylogenetic Tree Building. *Mol Biol Evol* **27**, 221–224 (2010).
34. F. Ronquist, J. P. Huelsenbeck, MrBayes 3: Bayesian phylogenetic inference under mixed models. *Bioinformatics* **19**, 1572–1574 (2003).
35. S. Kumar, G. Stecher, K. Tamura, MEGA7: Molecular Evolutionary Genetics Analysis Version 7.0 for Bigger Datasets. *Mol Biol Evol* **33**, 1870–1874 (2016).
36. S. Bensch, O. Hellgren, J. Pérez-Tris, MalAvi: a public database of malaria parasites and related haemosporidians in avian hosts based on mitochondrial cytochrome lineages *Molecular Ecology Resources* **9**, 1353–1358 (2009).
37. N. Puillandre, S. Brouillet, G. Achaz, ASAP: assemble species by automatic partitioning. *Molecular Ecology Resources* **21**, 609–620 (2021).
38. C. Drummond *et al.*, Stability and detection of nucleic acid from viruses and hosts in controlled mosquito blood feeds. *Plos One* **15**, (2020).

Supplementary Table 1. Composition of mosquitoes collected at altitude (120-290 m above ground)

No.	Species	Count	Comments
1	***Ad. africana***	1	
2	***Ae. aegypti***	2	May represent contamination during panel processing: both specimens were collected on the same panel at the 1st month of operation of a new team
3	***Ae. argenteopunctatus***	24	
4	***Ae. bromeliae***	2	
5	***Ae. circumluteolus***	12	
6	***Ae. dentatus***	1	
7	***Ae. fowleri***	10	
8	***Ae. mcintoshi***	10	
9	***Ae. quasiunivittatus***	23	
10	***Ae. sp. MBI-61***	1	
11	***Ae. sp. MBI-62***	2	
12	***An. cf. rivulorum***	1	
13	***An. coluzzii***	2	
14	***An. coustani***	12	
15	***An. funestus***	1	May represent contamination during panel processing: a singe specimen that is recorded for the first time in altitude. Needs verification.
16	***An. gambiae s.l.***	4	May represent Anopheles coluzzii or Anopheles gambiae s.s. rather than a new species: molecular ID has failed repeatedly
17	***An. gambiae s.s.***	1	
18	***An. longipalpis***	1	
19	***An. pharoensis***	8	
20	***An. pretoriensis***	2	
21	***An. rufipes***	6	
22	***An. squamosus***	20	
23	***Cq. ghana sp. 1***	2	
24	***Cq. metallica***	36	
25	***Cq. sp. MBI-01***	1	
26	***Cq. sp. MBI-03***	1	
27	***Cx. MBI-03***	6	
28	***Cx. MBI-18***	6	
29	***Cx. annulioris***	5	
30	***Cx. antennatus***	18	
31	***Cx. bitaeniorhynchus***	4	
32	***Cx. cf. watti MAFP5.C5***	92	
33	***Cx. cinereus***	6	
34	***Cx. decens***	11	
35	***Cx. duttoni***	1	
36	***Cx. ghana sp. 1***	7	
37	***Cx. ghana sp. 2***	3	
38	***Cx. inconspicuosus***	1	May be a closely related species
39	***Cx. mali sp. 4***	6	
40	***Cx. mali sp. 5***	1	
41	***Cx. neavei***	18	
42	***Cx. nebulosus***	17	
43	***Cx. perexiguus***	176	
44	***Cx. poicilipes***	7	
45	***Cx. sp. KHH5***	29	
46	***Cx. sp. MBI-65***	1	
47	***Cx. sp. MBI-66***	1	
48	***Cx. sp. MBI-68***	1	
49	***Cx. univittatus***	29	Was also referred to as *Cx. sp. M63YA*
50	***Cx. univittatus B***	3	
51	***Cx. watti***	321	
52	***Er. sp. MBI-01***	3	
53	***Lu. tigripes***	3	
54	***Ma. africana***	1	
55	***Ma. sp. MBI-60***	1	
56	***Ma. uniformis***	4	
57	***Mi. mediolineata***	2	
58	***Mi. mimomyiaformis***	6	
59	***Ur. alboabdominalis***	8	
60	***Ur. connali***	7	
61	***Ur. ghana sp. 1***	3	
	Culicidae	5	May contain additional species
	Culicinae	246	Failed to produce PCR products or quality mtCOI sequence. May contain additional species
	Anophelinae	2	Failed to produce PCR products or quality mtCOI sequence. May contain additional species
	Total mosquitoes	1247	Few preseved in 80% ethanol or on silica gel (not in RNAlater) were not subjected to RNA analyses

Supplementary Table 2. Mosquito sex composition by species in aerial collections (pooling species with N<10, see methods text)

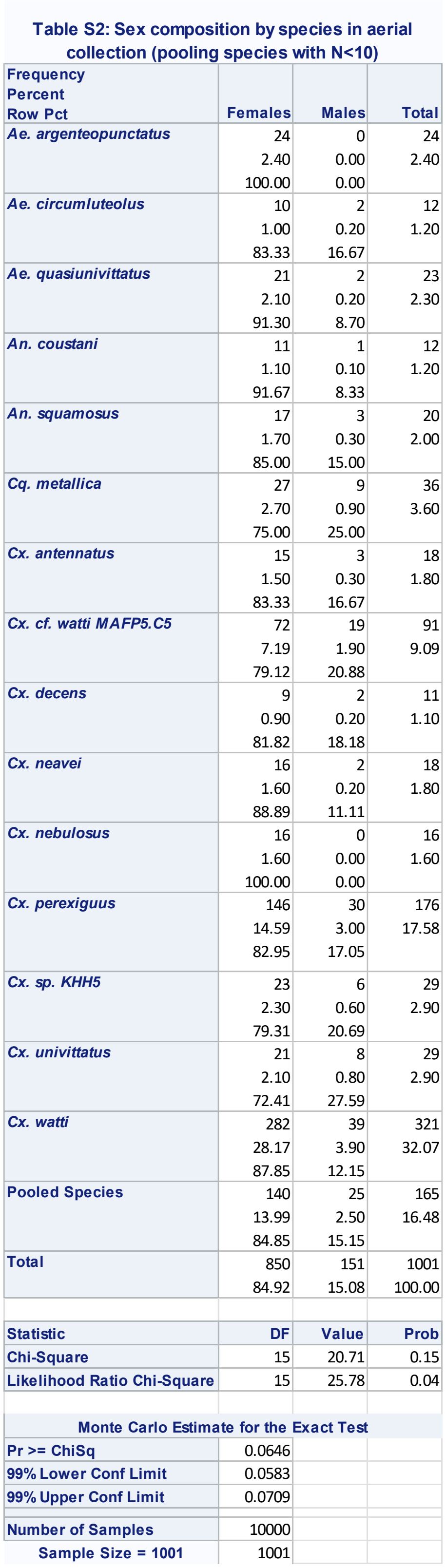

Table S2: Sex composition by species in aerial collection (pooling species with N<10)

Frequency Percent Row Pct	Females	Males	Total
Ae. argenteopunctatus	24	0	24
	2.40	0.00	2.40
	100.00	0.00	
Ae. circumluteolus	10	2	12
	1.00	0.20	1.20
	83.33	16.67	
Ae. quasiunivittatus	21	2	23
	2.10	0.20	2.30
	91.30	8.70	
An. coustani	11	1	12
	1.10	0.10	1.20
	91.67	8.33	
An. squamosus	17	3	20
	1.70	0.30	2.00
	85.00	15.00	
Cq. metallica	27	9	36
	2.70	0.90	3.60
	75.00	25.00	
Cx. antennatus	15	3	18
	1.50	0.30	1.80
	83.33	16.67	
Cx. cf. watti MAFP5.C5	72	19	91
	7.19	1.90	9.09
	79.12	20.88	
Cx. decens	9	2	11
	0.90	0.20	1.10
	81.82	18.18	
Cx. neavei	16	2	18
	1.60	0.20	1.80
	88.89	11.11	
Cx. nebulosus	16	0	16
	1.60	0.00	1.60
	100.00	0.00	
Cx. perexiguus	146	30	176
	14.59	3.00	17.58
	82.95	17.05	
Cx. sp. KHH5	23	6	29
	2.30	0.60	2.90
	79.31	20.69	
Cx. univittatus	21	8	29
	2.10	0.80	2.90
	72.41	27.59	
Cx. watti	282	39	321
	28.17	3.90	32.07
	87.85	12.15	
Pooled Species	140	25	165
	13.99	2.50	16.48
	84.85	15.15	
Total	850	151	1001
	84.92	15.08	100.00

Statistic	DF	Value	Prob
Chi-Square	15	20.71	0.15
Likelihood Ratio Chi-Square	15	25.78	0.04

Monte Carlo Estimate for the Exact Test

Pr >= ChiSq	0.0646
99% Lower Conf Limit	0.0583
99% Upper Conf Limit	0.0709
Number of Samples	10000
Sample Size = 1001	1001

Supplementary Table 3. Female mosquito gonotrophic state composition by species in aerial collections (pooling species with N<10, see methods text)

Table S3: Fraction of gravid females in aerial collection

Frequency Percent Row Pct	G	U	Total
Ae. argenteopunctatus	12	12	24
	1.44	1.44	2.87
	50.00	50.00	
Ae. circumluteolus	1	9	10
	0.12	1.08	1.20
	10.00	90.00	
Ae. quasiunivittatus	11	10	21
	1.32	1.20	2.51
	52.38	47.62	
An. coustani	4	5	9
	0.48	0.60	1.08
	44.44	55.56	
An. squamosus	11	6	17
	1.32	0.72	2.04
	64.71	35.29	
Cq. metallica	10	16	26
	1.20	1.92	3.11
	38.46	61.54	
Cx. antennatus	8	7	15
	0.96	0.84	1.80
	53.33	46.67	
Cx. cf. watti MAFP5.C5	23	42	65
	2.75	5.03	7.78
	35.38	64.62	
Cx. decens	4	4	8
	0.48	0.48	0.96
	50.00	50.00	
Cx. neavei	9	7	16
	1.08	0.84	1.92
	56.25	43.75	
Cx. nebulosus	6	9	15
	0.72	1.08	1.80
	40.00	60.00	
Cx. perexiguus	93	55	148
	11.14	6.59	17.72
	62.84	37.16	
Cx. sp. KHH5	13	11	24
	1.56	1.32	2.87
	54.17	45.83	
Cx. univittatus	6	15	21
	0.72	1.80	2.51
	28.57	71.43	
Cx. watti	99	184	283
	11.86	22.04	33.89
	34.98	65.02	
PooSpecies	55	78	133
	6.59	9.34	15.93
	41.35	58.65	
Total	365	470	835
	43.71	56.29	100.00

Statistic	DF	Value	Prob
Chi-Square	15	46.7075	<.0001
Likelihood Ratio Chi-Squ	15	47.6732	<.0001

Monte Carlo Estimate for the Exact Test			
Pr >= ChiSq	<.0001		
99% Lower Conf Limit	<.0001		
99% Upper Conf Limit	0.0005		
Number of Samples	10000		
Sample Size = 836	835		

Table S4. Infection rates of high-flying mosquitoes with insect-specific viruses and with non-mosquito-borne pathogens (e.g., *Trypanosoma theileri* and *Haemoproteus coraciae*) that probably reflects exposure during blood-feeding. The nucleic acids persist (at detection levels) 36-48 hours post bloodfeeding (*38*).

Microbe	Overall^a (N)	Method	Natural Host/Vector
Insect specific flaviviruses	1.1% (11/1,002)	Pan-Flavivirus PCR	Mosquito-specific
Barkedji virus	0.1% (1/1,002)	Metagenomics	Mosquito-specific
Anopheles flavivirus variant 1	0.1% (1/1,002)	Metagenomics	Mosquito-specific
Flavivirus-like endogenous virus	0.2% (2/1,002)	Metagenomics + Sanger	Mosquito-specific
Nienokue virus	0.5% (5/1,002)	Metagenomics + Sanger	Mosquito-specific
Mercado virus	0.1% (1/1,002)	Metagenomics	Mosquito-specific
Quang Binh virus	0.1%(1/1,002)	Metagenomics	Mosquito-specific
Other Insect-specific viruses^b			
Hameenlinna phasivirus	2.1% (1/48)	Metagenomics	Mosquito-specific
Aedes aegypti To virus 2	4.2% (2/48)	Metagenomics	Mosquito-specific
Zeya Brooke Chaq-like virus	2.1% (1/48)	Metagenomics	Mosquito-specific
Verdadero virus	2.1% (1/48)	Metagenomics	Mosquito-specific
Spilikins virus	2.1% (1/48)	Metagenomics	Mosquito-specific
Orbis virgavirus	2.1% (1/48)	Metagenomics	Mosquito-specific
Mos8Chu0 chuvirus	2.1% (1/48)	Metagenomics	Mosquito-specific
Culex mosquito virus 4	2.1% (1/48)	Metagenomics	Mosquito-specific
Broome reo-like virus 1	2.1% (1/48)	Metagenomics	Mosquito-specific
XiangYun mono-chu-like virus 7	6.3% (3/48)	Metagenomics	Mosquito-specific
Aedes binegev-like virus 2	2.1% (1/48)	Metagenomics	Mosquito-specific
Osterfarnebo virus	4.2% (2/48)	Metagenomics	Mosquito-specific
Culex pipiens-associated Tunisia virus	2.1% (1/48)	Metagenomics	Mosquito-specific
Mole Culex virus	2.1% (1/48)	Metagenomics	Mosquito-specific
Gysinge virus	4.2% (2/48)	Metagenomics	Mosquito-specific
Environmental Rhabdovirus	2.1% (1/48)	Metagenomics	Mosquito-specific
Biggie virus	2.1% (1/48)	Metagenomics	Mosquito-specific
Atrato-partiti like virus 1	2.1% (1/48)	Metagenomics	Mosquito-specific
Hubei virga-like virus 2	2.1% (1/48)	Metagenomics	Mosquito-specific
Forneby virus	2.1% (1/48)	Metagenomics	Mosquito-specific
Zhejiang mosquito virus 3	2.1% (1/48)	Metagenomics	Mosquito-specific
Haemosproida (excl. Plasmodium spp.)			Vertebrates/Biting midges
- *Haemoproteus coraciae*	0.2% (2/1006)	Sanger	Birds/biting midges
Trypanosomatida			
- *Trypanosoma theileri*	6.3 (3/48)	Metagenomics	Bovids, Cervids/biting flies
- *Paratrypanosoma confusum*	14.6 (7/48)	Metagenomics	Bovids, Cervids/biting flies
- *Trypanosoma* sp. 1	2.1% (1/48)	Metagenomics	Vertebrates/arthropods
- *Trypanosoma* sp. 2	2.1% (1/48)	Metagenomics	Vertebrates/arthropods

[a] Infection rate by mosquito (regardless of body part and including whole body mosquitoes) considering Sanger sequencing and metagenomics

[b] Infection was detected and confirmed by metagenomics after mosquito was detected as positive to flaviviruses

Table S5. Primers used for pathogen and mosquito detection and identification.

Pathogen-target	Gene	Primers/Probe	Sequence 5'-3'	Type of PCR	Sequenced amplicon size (bp)	Ref
Orthoflavivirus	NsP5	Flavi_F	TACAACATGATGGGAAAGAGAGAGAARAA	RT-qPCR with melting curve	NA	Vina-Rodriguez et al. 2017
		Flavi_R	GTGTCCCAKCCRGCTGTGTCATC			
Alphavirus	nsP4	Alpha_F	GIAAYTGYAAYGTIACICARATG		NA	
		Alpha_R	GCRAAIARIGCIGCIGCYTYIGGICC			
Orthoflavivirus	NsP5	FLAVI1-F	GCATCTAYAWCAYNATGGG	Nested PCR	~960 bp	Vazquez et al. 2012
		FLAVI1-R	CCANACNYNRTTCCANAC			
		FLAVI2-F	GCNATNTGGTWYATGTGG			
		FLAVI2-R	CATRTCTTCNGTNGTCATCC			
Plasmodium	COI	Plasmo_cox_15_F	AGGAACTCGACTGGCCTACA	qPCR	NA	Mediannikov et al. 2013
		Plasmo_cox_16_R	CCAGCGACAGCGGTTATACT			
		Plasmo-cox_P	6FAM-CGAACGCTTTTAACGCCTGACATGG -TAMRA			
	Cyt B	HAEMF	ATGGTGCTTTCGATATATGCATG	Nested PCR	~477 bp	Hellgreen et al. 2004
		HAEMR2	GCATTATCTGGATGTGATAATGGT			
		HaemNFI	CATATATTAAGAGAAITATGGAG			
		HaemNR3	ATAGAAAGATAAGAAATACCATTC			
		DW4	TGTTTGCTTGGGAGCTGTAATCATAATGTG		~799 bp	Templeton et al. 2016
		DW2	TAATGCCTAGACGTATTCCTGATTATCCAG			
		NCYBINR	CTTGTGGTAATTGACATCCAATCC			
		NCYBINF	TAAGAGAATTATGGAGTGGATGGTG			
Filaria	28s rRNA	qFil-28S-F	TTGTTTGAGATTGCAGCCCA	qPCR	NA	Laidoudi et al. 2020
		qFil-28S-R	GTTTCCATCTCAGCGGTTTC			
		qFil-28S-P	6FAM-CAAGTACCGTGAGGGAAAGT-TAMRA			

	COI	Fwd.957 Rwd.1465	ATRGTTTATCAGTCTTTTTTTATTGG GCAATYCAAATAGAAGCAAAAGT	PCR	~509 bp	
Mosquito	COI	LCO1490 HCO2198	GGTCAACAAATCATAAAGATATTGG TAAACTTCAGGGTGACCAAAAAATCA	PCR	~658 bp	Folmer et al 1994

Acronyms:

COI: Cytochrome c oxidase I (COX1)

Cyt-b: Cytochrome B

NsP: Nonstructural protein

qPCR: real-time(quantitative) PCR

RT-qPCR: reverse transcriptase quantitative PCR

Sequence amplicon sizes only for PCR or RT-PC